Rare Earth Elements Variations in a Hyperacid Crater Lake and Their Relations With Changes in Phreatic Activity, Physico-Chemical Parameters, and Chemical Composition: The Case of Poás Volcano (Costa Rica)

Sabrina Pappaterra[1], Claudio Inguaggiato[2,3]*, Dmitri Rouwet[3], Raúl Mora-Amador[4], Carlos Ramírez-Umaña[5], Gino González[3,4,6], Lorenzo Brusca[7], Loic Peiffer[2], Gilles Levresse[8] and Sergio Bellomo[7]

- [1]Posgrado en Ciencias de La Tierra, Centro de Investigación Científica y de Educación Superior de Ensenada, Baja California (CICESE), Ensenada, Mexico
- [2]Departamento de Geología, Centro de Investigación Científica y de Educación Superior de Ensenada, Baja California (CICESE), Ensenada, Mexico
- [3]Istituto Nazionale di Geofisica e Vulcanologia, Sezione di Bologna, Bologna, Italy
- [4]Volcanes Sin Fronteras, San José, Costa Rica
- [5]Servicio Geológico Ambiental de Costa Rica (SeGeoAm), San José, Costa Rica
- [6]Dipartimento di Scienze Della Terra e Geoambientali, Università Degli Studi di Bari Aldo Moro, Bari, Italy
- [7]Istituto Nazionale di Geofisica e Vulcanologia, Sezione di Palermo, Palermo, Italy
- [8]Centro de Geociencias, UNAM, Querétaro, Mexico

Decades of geochemical monitoring at active crater lakes worldwide have confirmed that variations in major elements and physico-chemical parameters are useful to detect changes in volcanic activity. However, it is still arduous to identify precursors of single phreatic eruptions. During the unrest phase of 2009–2016, at least 679 phreatic eruptions occurred at the hyperacid and hypersaline crater lake Laguna Caliente of Poás volcano (Costa Rica). In this study, we investigate the temporal variations of Rare Earth Elements (REE) dissolved in Laguna Caliente in order to 1) scrutinize if they can be used as a new geochemical tool to monitor changes of phreatic activity at hyperacid crater lakes and 2) identify the geochemical processes responsible for the variations of REE concentrations in the lake. The total concentration of REE varies from 950 to 2,773 μg kg^{-1}. $(La/Pr)_{N\text{-local rock}}$ ratios range from 0.93 to 1.35, and Light REE over Heavy REE $(LREE/HREE)_{N\text{-local rock}}$ ratios vary from 0.71 to 0.95. These same parameters vary in relation to significant changes in phreatic activity; in particular, the $(La/Pr)_{N\text{-local rock}}$ ratio increases as phreatic activity increases, while that of $(LREE/HREE)_{N\text{-local rock}}$ decreases when phreatic activity increases. REE concentrations and their ratios were compared with the variations of major elements and physico-chemical parameters of the lake. Calcium versus $(La/Pr)_{N\text{-local rock}}$ and versus $(LREE/HREE)_{N\text{-local rock}}$ ratios show different trends compared to the other major elements (Na, K, Mg, Al, Fe, SO_4, and Cl). Moreover, a higher loss of Ca (up to 2,835 ppm) in lake water was found with respect to the loss of Al, K, and Na. This loss of Ca is argued to be due to gypsum precipitation, a process corroborated by the mass balance calculation simulating the precipitation of gypsum and the contemporaneous removal of REE from the lake water. The observed relations between REE, changes in phreatic activity, and the parameters commonly used for the monitoring of hyperacid volcanic lakes encourage investigating more on the temporal and cause-effect relationship between REE dynamics and changes in phreatic activity at crater lake-bearing volcanoes.

1 Introduction

Volcanic areas are often characterized by the presence of lakes that fill the summit crater area (Manville, 2015). The chemical composition of volcanic lakes mainly depends on 1) the fluid input

from the underlying magmatic-hydrothermal system, 2) evaporation, meteoric precipitation, and infiltration, 3) dissolution of volcanic rocks, and 4) the precipitation of secondary minerals (Delmelle and Bernard, 1994; van Hinsberg et al., 2010; Varekamp, 2015). The combination of these factors leads to the genesis of fluids that span from dilute meteoric waters to hyperacid and hypersaline waters (Varekamp et al., 2000). Following Pasternack and Varekamp (1997), neutral-dilute volcanic waters are commonly associated with "no activity lakes," while hot hyperacid brines with high Total Dissolved Solids (TDS) are associated with "peak activity lakes".

The major hazards commonly associated with active crater lakes are 1) limnic gas bursts (Rouwet, 2021 and references therein) and 2) phreatic and phreatomagmatic eruptions (Barberi et al., 1992; Christenson, 2000; Christenson et al., 2010; de Moor et al., 2016; Rouwet et al., 2017; Stix and de Moor, 2018); the latter is also often responsible for the explosive ejection of the lake water to create 3) lahars on the volcano flanks (Kilgour et al., 2010; Manville, 2015). Stix and de Moor (2018) investigated the role of the magmatic contribution to phreatic eruptions, analyzing data from six different volcanic hydrothermal systems where phreatic activity is reported. They propose a model that includes two end-member types of phreatic eruptions named "phreato-vulcanian" and "phreato-surtseyan"; their variability is mainly related to the different depths and the different sealing characteristics of the hydrothermal system. The phreato-vulcanian type is more vigorous because of the features of the hydrothermal system, which is deeper and sealed and fed by magmatic gases that generate overpressure. The phreato-surtseyan type, on its turn, is characteristic of systems with open vents and a hydrothermal system close to the surface where the water is vaporized by the magmatic gases. In some conditions, a volcano can exhibit both types of phreatic eruptions, as in the case of Poás (Costa Rica) and Ruapehu (New Zealand) volcanoes (Stix and de Moor, 2018).

Since volcanic lakes represent the intersection of the magmatic-hydrothermal system of a volcano and the surface (Rowe et al., 1992b; Christenson and Tassi, 2015), they offer a "touchable object" and hence a unique opportunity to scrutinize the state of volcanic activity (Rouwet et al., 2017). For various decades, researchers have been looking for a useful tool to identify signals that precede phreatic eruptions at crater lakes; hence, the importance of volcanic lake monitoring is related to the possibility of recognizing short- and long-term signals, likely associated with volcanic hazards, to mitigate the risk (Rymer et al., 2009). The combination of various geophysical and geochemical methods, like microgravity, seismicity, electromagnetism, and gas monitoring, represents a useful approach for the study of sub-surface processes at active volcanoes (Brown et al., 1991; Rymer et al., 2009; Zlotnicki et al., 2009; de Moor et al., 2019). A common monitoring approach tracks the variations over the time of major elements and physico-chemical parameters of crater lake waters (Rowe et al., 1992b; Varekamp et al., 2000; Christenson, 2000; Ohba et al., 2008; Varekamp et al., 2009; Agusto and Varekamp, 2016; Rouwet et al., 2017, 2019). The results obtained investigating the geochemistry of various hyperacid volcanic lakes worldwide are consistent and show that mainly pH, temperature, and some anions and cations concentrations such as SO_4, Cl, and Mg, and their ratios (SO_4/Cl, and Mg/Cl) may be good indicators to monitor chemical changes of crater lake waters likely related to the degree of volcanic unrest (Giggenbach and Glover, 1975; Rowe et al., 1992b; Rouwet et al., 2019).

Since hyperacid volcanic fluids are more aggressive with respect to near-neutral and alkaline fluids during water-rock interaction, a higher amount of rock-derived elements, including Rare Earth Elements (lanthanides + yttrium; REE), is leached and mobilized (Michard, 1989; Lewis et al., 1997; Takano et al., 2004; Varekamp et al., 2009; van Hinsberg et al., 2010; Peiffer et al., 2011; Hikov, 2015; Inguaggiato et al., 2015; Varekamp, 2015; Inguaggiato et al., 2017; van Hinsberg et al., 2017; Woitischek et al., 2017; Inguaggiato et al., 2018; Inguaggiato et al., 2020a; Inguaggiato et al., 2020b). The geochemical and economic importance of REE prompted to study them in a wide variety of environments, among which the fluids associated with volcanic areas, and especially volcanic crater

lakes (Kikawada et al., 2004; Takano et al., 2004; Varekamp, 2015; van Hinsberg et al., 2017; Inguaggiato et al., 2018; Inguaggiato et al., 2020a; Inguaggiato et al., 2020b; van Hinsberg et al., 2020). Consequently to the increasing knowledge of the geochemical behavior of REE, it is possible to develop several applications using REE as geochemical tracers of fluid-rock interaction in active volcanic systems.

Inguaggiato et al. (2018) investigated the geochemical processes that affect the pattern of REE at Laguna Caliente (2006–2009), the active hyperacid and hypersaline crater lake of Poás volcano in Costa Rica, the study object of this investigation. Mainly, water-rock interaction processes, congruent dissolution of the andesitic rocks and the precipitation of secondary minerals like gypsum, seem to control the amount of REE dissolved in crater lake water (Inguaggiato et al., 2018). These processes induce changes in the REE concentrations and control the relative proportion among them over time.

Despite the increasing investigation and the improvement of modern and sophisticated monitoring techniques, it is still difficult to identify precursors for single phreatic eruptions. Moreover, sampling the crater lake of an active volcano is arduous and dangerous, especially during periods of increased activity (i.e., phreatic eruptions). In this study, we had the chance to collect numerous water samples at Poás's Laguna Caliente when hundreds of phreatic eruptions occurred and to experience the potential effectiveness of REE in hyperacid volcanic lakes as a new possible geochemical indicator of changes in phreatic activity. We investigated if the variations of REE in Laguna Caliente could be connected to the main changes of phreatic activity, here represented by the occurrence of 679 phreatic eruptions during the period 2009–2016, and if they could be connected with the temporal variations of the geochemical indicators previously used to monitor Laguna Caliente volcanic activity (Rouwet et al., 2017; Rouwet et al., 2019). Our investigation aims to 1) improve the knowledge on the processes that control the REE variations in hyperacid crater lakes over time and their relations with the changes in volcanic activity, 2) compare the REE variations with the more classic geochemical parameters used to monitor volcanic activity, and 3) prove the usefulness of REE as a possible geochemical tool sensitive to changes in volcanic activity. Laguna Caliente was sampled with an average sampling frequency of 40 days from June 2009 to February 2016. This period is included within the 2006–2016 phreatic eruption cycle but is before the phreatomagmatic activity in 2017 (Mora-Amador et al., 2019a). Here, we compare the variations of REE dissolved in the Laguna Caliente water with the 1) evolution of the volcanic activity of Poás, manifested by 679 phreatic eruptions, 2) variations of physico-chemical parameters, and 3) variations of major elements chemical composition and their ratios in lake water. A key focus will be to describe the REE behavior in the Poás hyperacid crater lake during the phreatic activity and test it as a potential volcanic monitoring tool, in addition to the already proven and well-known geochemical pre-eruption indicators in both Poás lake and other volcanic hydrothermal systems worldwide (i.e., physico-chemical parameters and major elements).

2 Background Information

2.1 Geological Setting

Poás (10°11′26″N 84°13′56″W) is a stratovolcano in Costa Rica that belongs to the Central Volcanic Range (CVR; Ruíz et al., 2019). It is composed of various volcanic structures, such as the composite cones at its top, Von Frantzius, Botos, and the Main Crater, that represents the spot of the historical activity (Prosser and Carr, 1987; Mora-Amador et al., 2019a). The main hydrological features at Poás volcano include 1) a hyperacid crater lake, named Laguna Caliente, that fills the active Main Crater, 2) a freshwater lake hosted at Botos cone, called Laguna Botos, and 3) acid springs and streams at the north-western flank of the volcano, which are part of the Río Agrio drainage basin and that arguably represent the seepage out of Laguna Caliente (Rowe et al., 1995; Sanford et al., 1995).

Poás is one of the most active volcanoes of the Central American Volcanic Arc. Its activity is mostly characterized by phreatic and phreatomagmatic eruption cycles at the Main Crater during the last 200 years (Alvarado, 2009; Ruíz et al., 2010; Mora-Amador et al., 2019a; Rouwet et al., 2019; Vannucchi and Morgan, 2019). The maximum age of the deposits that compose Poás volcano is about 600 ka. The lavas have a geochemical composition resulting from a fractional crystallization that generated products ranging from basalts to dacites; andesites and basaltic andesites are the most common products (Ruíz et al., 2010, 2019).

The chemical composition of Laguna Caliente is typical of "gas-dominated" crater lakes, characterized by an extremely low (hyperacid) pH and very high TDS values, with SO_4, Cl, and F as the most dominant gas-derived anion solutes and Al and Fe as the most abundant cations (Rowe et al., 1992b, 1995; Martínez et al., 2000; Varekamp et al., 2000; Rouwet et al., 2014, 2017, 2019). Lake volume changed dynamically through time and these changes largely result from the input of meteoric precipitation and fluids at the lake bottom and the water loss caused by seepage and evaporation (Brown et al., 1989; Rowe et al., 1992a; Rouwet et al., 2017). Laguna Caliente has dried out various times during the last decades (1989–1994, 2017), inducing subaerial degassing of the fumaroles located at the bottom of the crater (Rowe et al., 1992a; Martínez et al., 2000; Rymer et al., 2009) and peculiar sulfur volcanism (Oppenheimer, 1992; Mora-Amador et al., 2019b).

2.2 Historical Activity at Poás Volcano

At the present day, Poás represents one of the most active volcanoes on Earth. Due to the dense vegetation, very few outcrops exist to reveal the deposits of the eruptions that occurred prior to the 19th century. A recent report about the historical eruptions at Poás volcano is available (Mora-Amador et al., 2019a). von Frantzius (1861) reported intense volcanic activity at Poás volcano in 1828 and in February 1834. Recent studies of the deposits enabled reconstructing the phreatic nature of the 1834 event, which involved blocks and bombs thrown out and pyroclastic flows (Mora-Amador et al., 2019a). The subsequent eruption was reported almost 80 years after, in 1910. It was a phreatomagmatic eruption characterized by fine ashfall. Phreatic activity is reported for the period between 1953 and 1955. In May 1953, a phreatomagmatic eruption, with some strombolian phases, took place, causing the expulsion of the crater lake and the extrusion of a lava dome characterized by fumarolic activity. The eruptive period extended until 1955 (Mora-Amador et al., 2019a) and produced an important change in morphology of the crater area (Brantley et al., 1987; Brown et al., 1989; Vaselli et al., 2003; Hilton et al., 2010; Fischer et al., 2015; Rouwet et al., 2019).

An earthquake swarm in 1986 signaled the start of an unrest phase. A powerful phreatic eruption in 1988 caused a lake level drop and full lake disappearance in 1989 (Rowe et al., 1992a; Oppenheimer, 1993). The phreatic activity continued until 1994, after which a decade of quiescence took over (Mora-Amador et al., 2019a). Since 1998, various changes have been observed in fumarolic activity: new fumarolic vents were formed and fumarolic activity migrated inside the Main Crater; changes in lake level and color were observed (Vaselli et al., 2003, 2019; Rouwet et al., 2017; Mora-Amador et al., 2019a). In December 2005, floating sulfur spherules with tails were present at the lake, an early-warning indicator of oncoming phreatic eruptions (Takano et al., 1994; Mora Amador et al., 2019b).

After more than a decade of quiescence, on March 24, 2006, the first phreatic eruption marked the beginning of 10 years of nearly continuous volcanic activity. During the period 2006–2016 (including the period of observation of the current study), more than 700 phreatic eruptions breached Laguna Caliente, peaking in frequency between 2010 and 2011 (de Moor et al., 2016; Rouwet et al., 2017; Rouwet et al., 2019). Prior to 2009, the activity was less intense; however, the first major phreatic event of the period occurred in September 2009. The frequency of eruptions had declined since 2014 to wane towards 2016 when an apparent stage of quiescence took over. Nevertheless, Poás culminated

into explosive phreatomagmatic activity on April 14, 2017, following a few days of intense geysering from new vents southwest outside Laguna Caliente (Mora-Amador et al., 2019a). The April 2017 phreatomagmatic eruption destroyed the 1955 lava dome to enlarge the crater lake basin that filled up after a period of sulfur volcanism at the dried-out lake bottom. On the day of writing (April 2021), Laguna Caliente is in a stage of medium activity (46°C); a new fumarolic field called "planicie de azufre" (sulfur plain) is located at the eastern shore of the lake. However, eruptive activity has not been reported since 2017.

3 Sampling and Analytical Methods

3.1 Sampling Methods, Data Provenance, and Their Analysis

Fifty-one aliquots of water were sampled at Laguna Caliente during the period between June 5, 2009, and February 23, 2016 (Figure 1). The sampling procedure and physico-chemical parameters are from Rouwet et al. (2017, 2019; Table 1). All the samples were filtered *in situ* using 0.45 µm Millipore filters and stored in HDPE bottles. Because of the extremely low pH values (~0), the samples were not acidified.

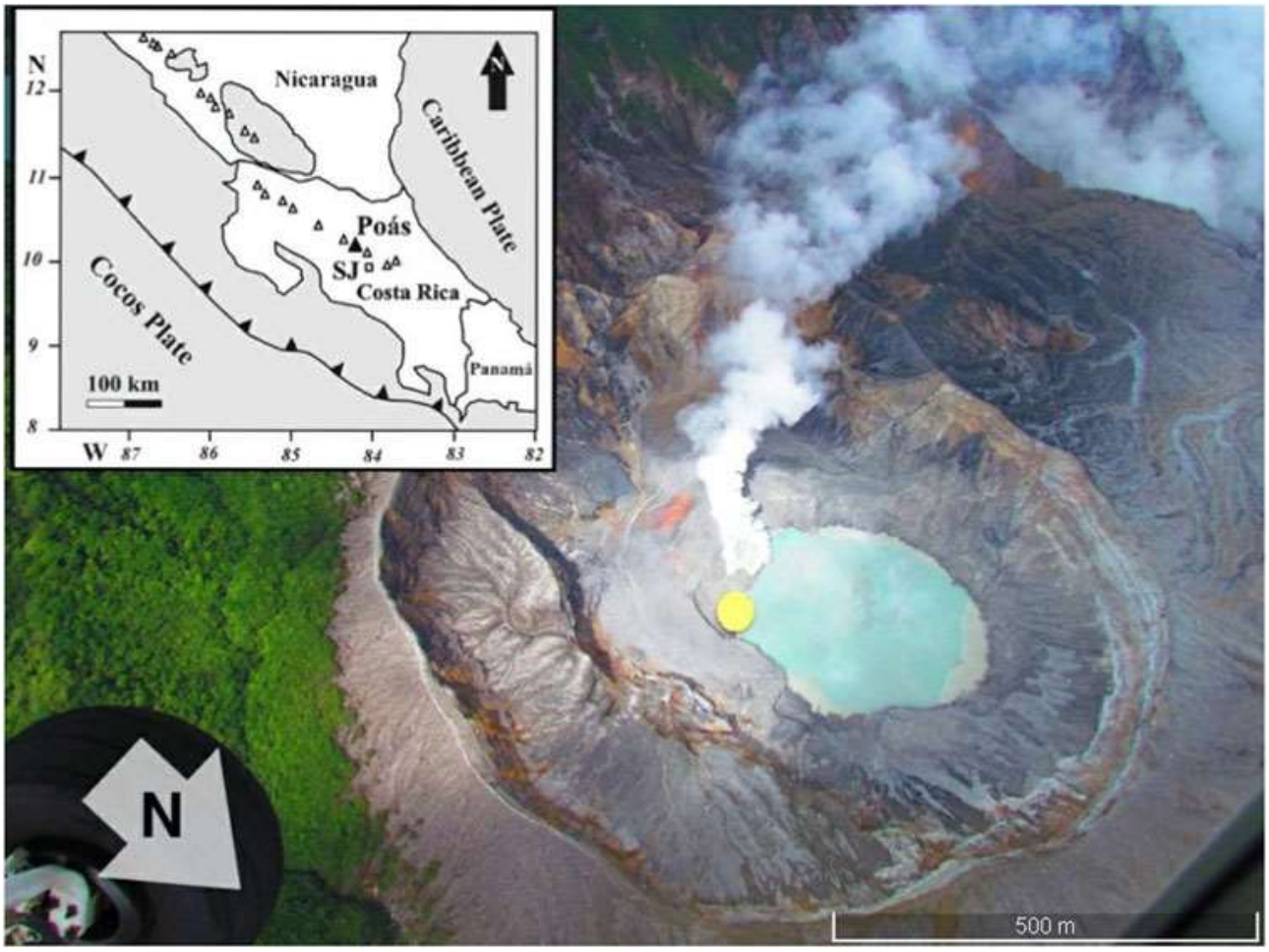

FIGURE 1. Map of the Cordillera Volcánica Central and location of Poás volcano, Costa Rica (black triangle) (Rouwet et al., 2017). Aerial photograph of Laguna Caliente (Poás volcano) and location of the sampling point "LD" at the dome (yellow dot). The photo was taken by Raúl Mora-Amador on 17/04/2012.

A comprehensive database of the 679 phreatic eruptions, which took place from June 2008 to June 2016, has been compiled based on data from scientific publications and public sources (Universidad de Costa Rica https://rsn.ucr.ac.cr; Observatorio Vulcanológico y Sismológico de Costa Rica, OVSICORI, 2021; Rouwet et al., 2017, Rouwet et al., 2019).

Phreatic eruptions are subdivided into three categories based on the column height: A) 2–50 m, B) 51–250 m, and C) >250 m (Mora-Amador, 2010; Rouwet et al., 2019). Moreover, a fourth category is here discriminated for all the eruptions without information about the column height ("N.D.": Not Defined).

3.2 Analytical and Laboratory Procedures

Major elements and physico-chemical parameters data are from Rouwet et al. (2017, 2019). REE analyses were carried out at INGV-Palermo using a Q-ICP-MS Agilent 7500 calibrated with a REE multi-element standard solution with 11 calibration points. The sample waters were diluted up to reach salinity around 0.6 g L^{-1}.

The sensitivity variation was monitored by three internal standards (^{103}Rh, ^{115}In, and ^{185}Re) to reach a final concentration of 8 µg L^{-1}.

Memory interferences between consecutive samples were reduced with a 60 s rinse using a 0.5% HCl and 2% HNO_3 solution plus a 60 s rinse using 2% HNO_3 solution. The analyses of three reference materials, SPS-SW1, SPS-SW2, and SLRS-4, were carried out to evaluate data accuracy. Each analysis is obtained by calculating the mean value of five replicates. The accuracy was usually better than 5%, and the average relative standard deviation (RSD) was calculated on five replicates and was mostly better than 7%.

4 Results

4.1. Stages of Phreatic Eruptive Activity

Almost 700 phreatic eruptions were observed and reported at Laguna Caliente between June 2008 and June 2016; however, it is likely that the real number of phreatic eruptions that occurred during this period is even higher. Our database counts 679 phreatic events (Figure 2; Supplementary Table 1). Approximately about ~62% of the total eruptions are "A" type eruptions, ~ 11% are "B" type eruptions, and only ~ 2% are "C" type eruptions, while the remaining ~ 25% are classified as "not determined" (ND).

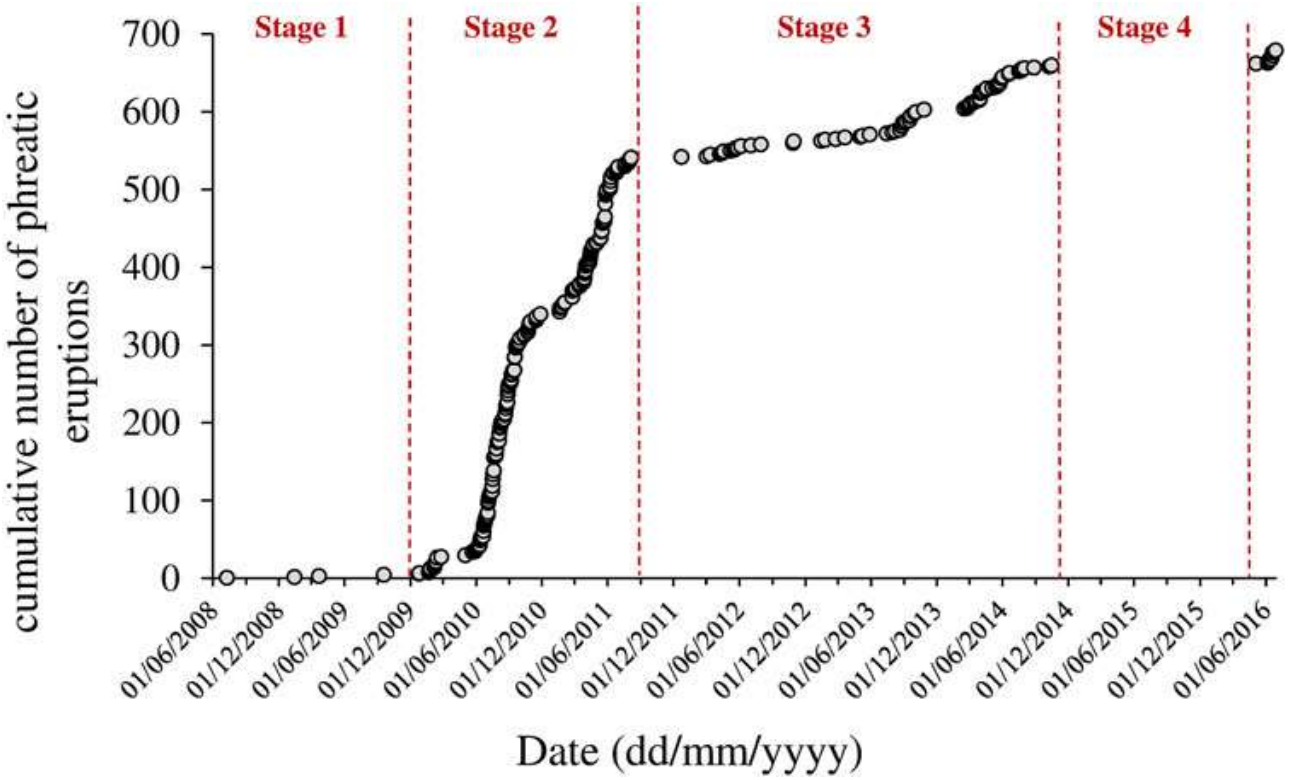

FIGURE 2. Cumulative number of phreatic eruptions vs. time. Four stages of activity are identified: 1) low frequency of phreatic eruptions, 2) high frequency of phreatic eruptions, 3) decline of phreatic eruptions, and 4) a period of quiescence.

Phreatic eruption intensity varies significantly during the time of observation. For the period between June 2008 and June 2016, the phreatic eruption cycle was subdivided into four stages characterized by 1) low phreatic activity, when only three "A" and one "C" type single eruptions occurred (June 2008–December 2009), 2) high frequency of phreatic eruptions (January 2010–August 2011, 535 phreatic eruptions), 3) declining number of phreatic events (September 2011–October 2014), and 4) a period of quiescence (November 2014–May 2016) that finished with the occurrence of 18 phreatic eruptions between May and June 2016. After a quiescent period following June 2016, Poás culminated in phreatomagmatic activity in April 2017 (the eruption is not included in the database of this investigation). These four distinct stages are better marked in Figure 2, where the cumulative number of phreatic eruptions is reported versus time. Almost all the multiple-eruptions days, which include at least a B or C eruption type, are between September 2009 and May 2012. After that, multiple eruptions B and C types were absent until mid-2014, when two multiple events, including B-type eruptions, took place and mid-2016, when a multiple event, including a B-type eruption, occurred.

4.2 Temporal Variations of REE

The REE were subdivided into two sub-groups, Light Rare Earth Elements (LREE; from La to Gd) and Heavy Rare Earth Elements (HREE; from Tb to Lu and Y). The concentrations of REE were normalized to the composition of the average local rock to easily compare the REE distribution with the andesitic rocks interacting with the fluids (Carr et al., 2013; Supplementary Figures 1A,B) and were subdivided into two groups: 1) samples belonging to stages 2 and 3 characterized by a more intense phreatic activity; 2) samples belonging to stages 1 and 4, characteristic of low phreatic activity. During the intense activity (stages 2 and 3), the patterns of REE are often characterized by different degrees of LREE depletion with respect to the HREE (Supplementary Figure 1A). On the

contrary, during low phreatic activity (stages 1 and 4), the patterns of REE do not show a pronounced LREE depletion and almost all the samples have similar trends that only differ for their absolute REE concentrations.

Total REE concentrations (∑REE) dissolved in the lake water change over time from 950 to 2,773 µg kg^{-1} (Table 2). ∑REE starts to increase prior to the high-frequency eruptive period starting in December 2009 and progressively increases throughout this high-frequency stage in 2010 and 2011 (Figure 3). Towards the end of 2011, the ∑REE started to decrease to reach the lowest values in 2016.

Sample number	Sample ID	Date	T (°C)	pH	Na	K	Ca	Mg	Al	Fe	Cl	SO_4	TDS	SO_4/Cl	Mg/Cl
1	22c	05/06/2009	53.6	−0.07	365	189	1,168	336	990	790	15,400	44,200	63	2.87	0.02
2	23c	16/06/2009	53.2	−0.09	350	154	1,222	340	1,260	630	15,700	46,700	66	2.97	0.02
3	24c	24/06/2009	52.5	−0.10	300	130	1,056	303	1,270	660	15,900	47,200	67	2.97	0.02
4	25c	01/07/2009	55.4	−0.11	314	134	983	316	1,340	700	16,300	48,500	69	2.98	0.02
5	26c	07/07/2009	52.4	−0.09	322	135	1,145	315	1,180	620	15,400	46,600	66	3.03	0.02
6	29c	31/07/2009	52.1	−0.15	321	140	1,134	322	1,270	650	17,000	52,800	74	3.11	0.02
7	30c	19/08/2009	57.0	−0.17	331	144	1,160	327	1,310	680	17,700	56,000	78	3.16	0.02
8	31c	08/09/2009	53.0	−0.15	332	140	1,191	337	1,260	670	17,000	54,100	75	3.18	0.02
9	32c	17/09/2009	57.0	−0.23	372	167	1,205	365	1,470	760	20,700	63,500	89	3.07	0.02
10	33c	25/11/2009	49.2	−0.24	382	172	1,124	373	1,840	1000	20,700	67,100	93	3.24	0.02
11	34c	09/12/2009	48.7	−0.22	397	164	865	399	1,700	950	19,500	63,800	88	3.27	0.02
12	36c	13/05/2010	53.0	−0.28	430	219	715	391	1,730	1,023	22,100	70,900	98	3.21	0.02
13	37c	03/06/2010	48.0	−0.27	454	233	743	415	1,770	1,033	21,600	70,700	97	3.27	0.02
14	38c	19/01/2011	–	−0.39	479	252	834	298	1,649	890	18,700	68,000	91	3.64	0.02
15	39c	22/02/2011	–	−0.40	487	286	687	269	1,428	764	19,000	70,200	93	3.69	0.01
16	41c	30/06/2011	–	−0.52	617	304	650	445	1,806	957	24,300	92,800	122	3.82	0.02
17	42c	06/07/2011	–	−0.52	746	322	569	458	2,286	1,302	24,500	92,900	123	3.79	0.02
18	43c	30/07/2011	–	−0.27	923	192	722	262	1,376	2,079	13,400	56,100	75	4.19	0.02
19	44c	10/08/2011	–	−0.55	642	379	543	435	2,138	1,234	29,900	122,300	158	4.09	0.01
20	45c	22/09/2011	61	−0.55	697	355	595	391	2,643	1,483	28,600	118,000	153	4.13	0.01
21	46c	13/10/2011	53	−0.49	566	307	687	347	2,074	1,103	26,400	106,900	138	4.05	0.01
22	47c	27/10/2011	60	−0.51	597	349	746	419	2,233	1,204	28,800	113,500	148	3.94	0.01
23	48c	27/12/2011	53	−0.34	426	277	920	276	1,704	900	18,800	79,300	103	4.22	0.01
24	49c	15/02/2012	56	−0.36	460	283	817	305	1,679	858	18,700	84,400	108	4.51	0.02
25	50c	21/03/2012	54	−0.35	524	277	706	241	1,680	857	18,700	81,500	104	4.36	0.01
26	51c	05/04/2012	49	−0.40	423	330	748	280	1,717	881	19,800	82,300	106	4.16	0.01
27	52c	26/04/2012	–	−0.36	340	345	884	304	1,920	840	18,800	80,300	104	4.27	0.02
28	53c	30/04/2012	–	−0.37	317	229	781	295	1,900	850	19,300	82,500	106	4.27	0.02
29	54c	29/08/2012	–	−0.37	323	331	765	281	1,840	840	19,000	84,500	108	4.45	0.01
30	55c	12/09/2012	–	−0.37	294	211	779	269	1,710	780	18,400	83,600	106	4.54	0.01
31	56c	26/09/2012	–	−0.37	316	287	726	266	1,760	800	17,900	81,700	104	4.56	0.01
32	57c	11/10/2012	–	−0.36	337	304	760	250	1,700	790	18,400	83,600	106	4.54	0.01
33	58c	10/01/2013	–	−0.24	265	181	785	236	1,450	690	14,300	64,400	82	4.50	0.02
34	59c	27/02/2013	–	−0.27	304	206	888	285	1,500	730	15,000	66,300	85	4.42	0.02
35	60c	20/03/2013	–	−0.27	291	198	854	277	1,520	740	16,600	67,800	88	4.08	0.02
36	61c	03/05/2013	46.1	−0.23	348	184	843	289	1,500	790	15,000	63,800	83	4.25	0.02
37	62c	08/05/2013	44.6	−0.29	318	232	810	286	1,560	780	16,400	70,600	91	4.30	0.02
38	63c	27/06/2013	47.4	−0.28	296	200	818	273	1,370	740	16,900	69,000	90	4.08	0.02
39	64c	04/09/2014	45.1	−0.26	234	149	857	217	1,240	710	25,500	70,500	99	2.76	0.01
40	65c	17/09/2014	47.7	−0.23	240	151	864	217	1,150	640	14,600	86,100	104	5.90	0.01
41	66c	24/09/2014	48.3	−0.22	228	147	966	220	1,130	630	13,700	64,900	82	4.74	0.02
42	67c	27/11/2014	34.6	−0.16	236	114	903	198	1,040	560	12,000	62,600	78	5.22	0.02
43	68c	13/04/2015	–	−0.03	216	89	788	178	890	500	9,200	44,300	56	4.82	0.02
44	69c	21/05/2015	34.6	−0.02	215	87	939	179	900	490	9,400	43,400	56	4.62	0.02
45	70c	14/07/2015	39.5	0.15	226	61	908	174	720	390	6,300	30,000	39	4.76	0.03
46	71c	26/08/2015	–	0.20	214	96	895	133	690	370	5,700	26,800	35	4.70	0.02
47	72c	07/10/2015	–	0.23	140	51	912	120	590	310	5,300	24,300	32	4.58	0.02
48	73c	18/11/2015	–	0.22	143	59	866	117	600	320	5,800	2,4900	33	4.29	0.02
49	74c	03/12/2015	–	0.18	163	57	907	125	650	490	9,900	28,200	40	2.85	0.01
50	75c	14/01/2016	–	0.16	172	54	979	132	630	350	6,400	28,600	37	4.47	0.02
51	76c	23/02/2016	–	0.26	118	35	495	102	530	280	5,100	22,400	29	4.39	0.02

TABLE 1. Major elements concentrations (mg L^{-1}), physico-chemical parameters, TDS (g L^{-1}) and major elements ratios (Rouwet et al., 2017, 2019).

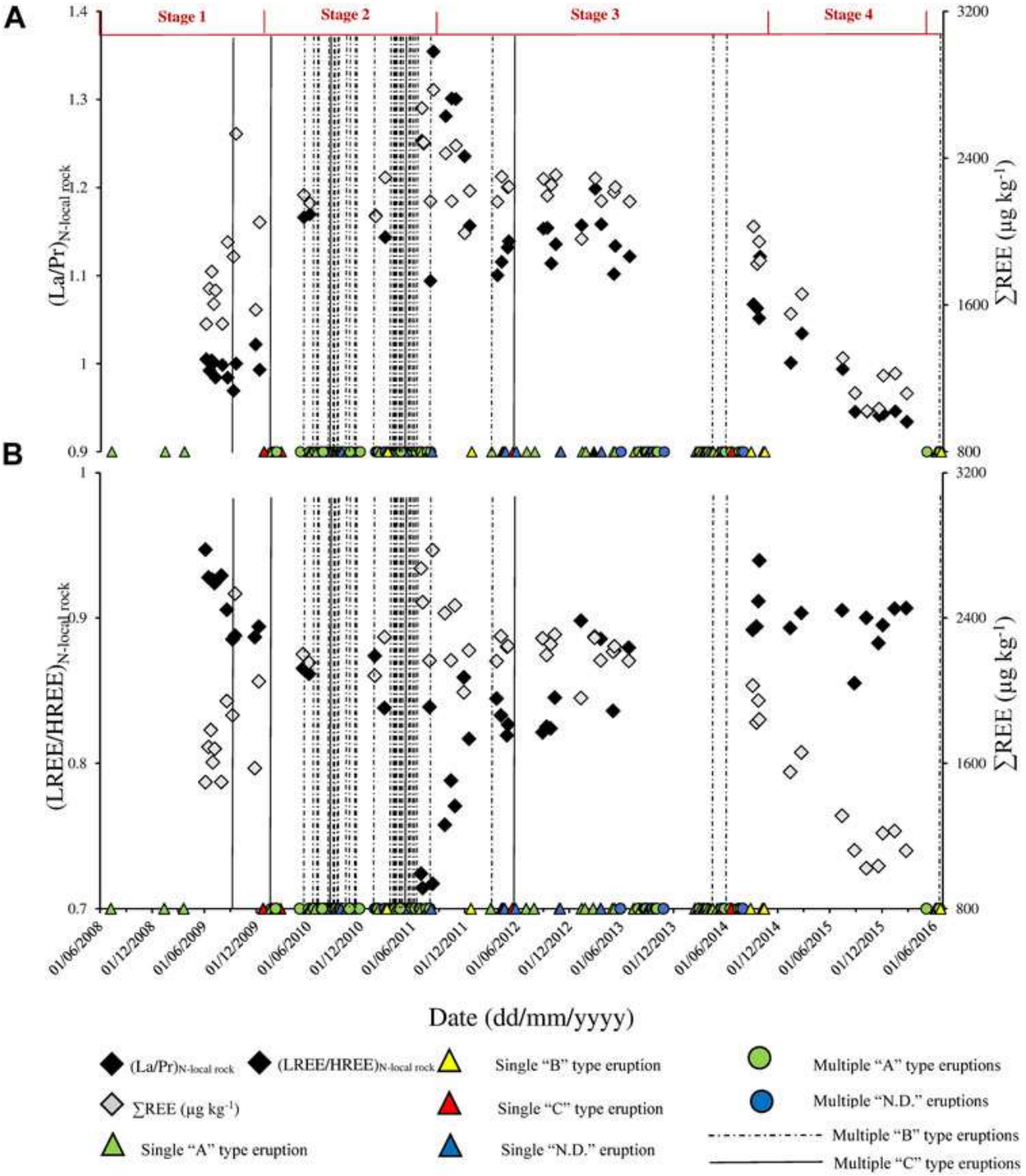

FIGURE 3. **(A)** $(La/Pr)_{N\text{-local rock}}$ and ∑ REE vs. time. **(B)** $(LREE/HREE)_{N\text{-local rock}}$ and ∑ REE vs. time.

Previous studies have already identified that in the hyperacid crater lakes of Poás (Costa Rica) and Kawah Ijen (Indonesia), gypsum precipitation can be responsible for the fractionation of REE dissolved in waters (Inguaggiato et al., 2018; Inguaggiato et al., 2020a; van Hinsberg et al., 2020). The distribution coefficients of REE, calculated between the REE in gypsum precipitated in the laboratory from the lake water and the REE dissolved in the lake water of Poás and Kawah Ijen crater lakes, demonstrate that LREE are preferentially scavenged by gypsum with respect to the HREE. Cerium, Pr, and Nd show higher distribution coefficients not only with respect to the HREE but also

with respect to the other LREE, including the neighboring elements La and Sm. This result shows that REE incorporation in gypsum decreases progressively from Nd to Lu, with La distribution coefficients that are mostly lower with respect to Ce, Pr, and Nd. Praseodymium often has the highest distribution coefficient and hence suggests preferential incorporation in the gypsum crystals during the precipitation process (Inguaggiato et al., 2018). Here, these previous findings $(La/Pr)_{N\text{-local rock}}$ and the $(LREE/HREE)_{N\text{-local rock}}$ ratios were considered to investigate the possible causes of temporal variations of REE in Poás crater lake water. Inguaggiato et al. (2018) suggested that the variations between LREE and HREE in the lake water can be affected by gypsum precipitation; we focused on the possibility that this process could also induce the variation of REE concentrations over time.

During the period of observation, $(La/Pr)_{N\text{-local rock}}$ and $(LREE/HREE)_{N\text{-local rock}}$ showed significant variations from 0.93 to 1.35 and from 0.71 to 0.95, respectively (Figure 4). The $(La/Pr)_{N\text{-local rock}}$ ratio was lower in mid-2009, when only a few eruptions have occurred (stage 1), and started to increase in early 2010 when eruptive activity was more intense and of higher frequency, to peak in September 2011 (stage 2). Afterward (early stage 3), $(La/Pr)_{N\text{-local rock}}$ decreased to remain stable between late 2011 and mid-2013 when the number of phreatic eruptions was considerably lower than that in the previous years. After the data gap between mid-2013 and late 2014, the $(La/Pr)_{N\text{-local rock}}$ ratio progressively decreased, starting from mid-2013 ratio values until the end of the time series (2016, stage 4), reaching similarly low values as those during stage 1 (2008–2009).

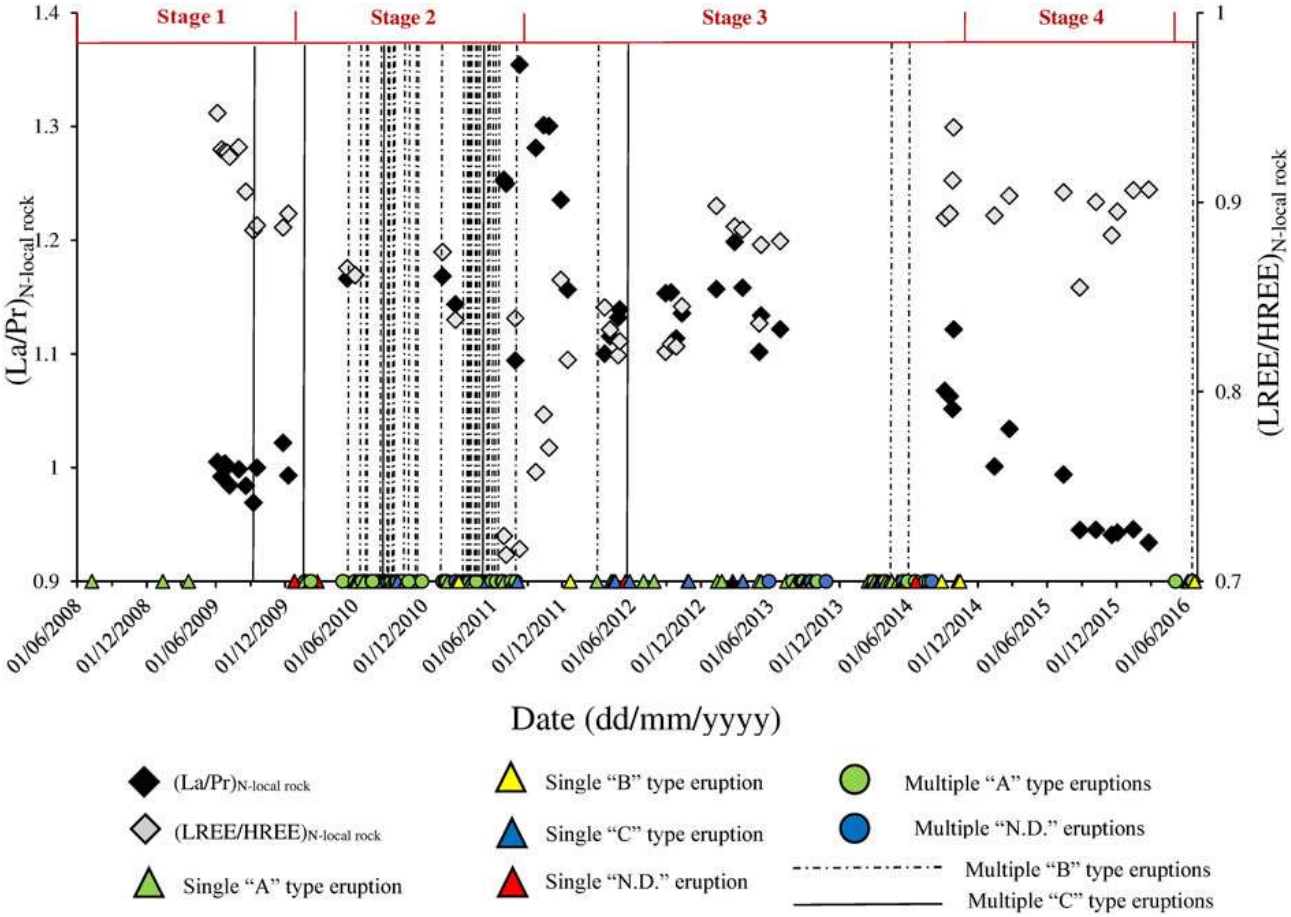

FIGURE 4. $(La/Pr)_{N\text{-local rock}}$ and $(LREE/HREE)_{N\text{-local rock}}$ vs. time.

The $(LREE/HREE)_{N\text{-local rock}}$ ratio shows a trend over time that is nearly opposite to the $(La/Pr)_{N\text{-local rock}}$ trend (Figure 4). The decreasing trend in stage 1 (2008–mid-2009) accelerates during the period of high-frequency phreatic activity (stage 2, 2010–2011). From late 2011 until 2013, the

$(LREE/HREE)_{N\text{-local rock}}$ ratio progressively increased, concurrently to the decrease in the frequency of phreatic eruptions. The ratio does not vary significantly from 2014 to 2016, with values comparable to the ones of 2009. Moreover, looking at mid-2009, we observed that the $(LREE/HREE)_{N\text{-local rock}}$ ratio started to decrease before the occurrence of the first multiple phreatic eruptions (stage 1, September 2009). The variations of $(La/Pr)_{N\text{-local rock}}$ and $(LREE/HREE)_{N\text{-local rock}}$ ratios are related to the major changes of volcanic activity, reaching the higher and the lower values, respectively, when the activity reaches a climax (stage 2, September 2011).

4.3 REE Versus Physico-Chemical Parameters and Chemical Composition

The $(La/Pr)_{N\text{-local rock}}$, $(LREE/HREE)_{N\text{-local rock}}$ ratios and eruptions data were compared to major element concentrations (Na, K, Mg, Ca, Al, Fe, SO_4, Cl), major element ratios (SO_4/Cl, Mg/Cl), physico-chemical parameters of the lake (pH, T), TDS values (Table 1), and the REE total amount (ΣREE; Table 2; Figures 3, 5–9, Supplementary Figures 2, 3).

Sample number	Sample ID	Date	La	Ce	Pr	Nd	Sm	Eu	Gd	Tb	Dy	Y	Ho	Er	Tm	Yb	Lu	∑REE	La/Pr	LREE/HREE
1	22c	05/06/2009	242	493	61	248	55	16	55	8	43	215	8	24	3	21	3	1,496	1.01	0.95
2	23c	16/06/2009	272	554	69	279	62	19	61	9	49	246	10	28	4	24	3	1,690	0.99	0.93
3	24c	24/06/2009	287	585	72	294	66	20	66	9	53	258	10	29	4	25	4	1,783	1.00	0.93
4	25c	01/07/2009	259	528	65	265	59	18	58	8	47	233	9	26	4	23	3	1,606	1.00	0.93
5	26c	07/07/2009	266	550	68	279	62	19	62	9	50	246	10	28	4	24	4	1,679	0.98	0.92
6	29c	31/07/2009	241	490	61	249	56	17	57	8	45	212	9	25	3	22	3	1,497	1.00	0.93
7	30c	19/08/2009	309	635	79	322	72	22	73	10	60	278	11	33	5	29	4	1,943	0.98	0.91
8	31c	08/09/2009	290	604	76	311	71	21	71	10	59	271	11	33	4	28	4	1,864	0.97	0.89
9	32c	17/09/2009	403	825	102	415	95	28	98	14	80	366	15	44	6	39	6	2,534	1.00	0.89
10	33c	25/11/2009	257	515	64	255	58	18	59	9	48	224	10	28	4	23	4	1,574	1.02	0.89
11	34c	09/12/2009	327	675	83	337	75	23	78	11	62	290	12	36	5	31	5	2,051	0.99	0.89
12	36c	13/05/2010	383	704	83	332	74	23	75	11	64	358	13	37	5	32	5	2,200	1.17	0.87
13	37c	03/06/2010	375	684	81	332	72	23	74	11	63	347	13	36	5	32	5	2,154	1.17	0.86
14	38c	19/01/2011	367	669	79	320	70	22	72	11	60	326	12	35	5	30	5	2,082	1.17	0.87
15	39c	22/02/2011	398	734	88	359	79	25	82	12	74	341	14	41	6	36	5	2,295	1.14	0.84
16	41c	30/06/2011	477	835	96	379	82	26	94	15	90	446	18	52	7	48	7	2,673	1.25	0.72
17	42c	06/07/2011	438	770	89	354	76	25	87	14	83	425	17	50	7	45	7	2,486	1.25	0.71
18	43c	30/07/2011	361	685	84	341	77	24	80	12	70	337	14	39	5	33	5	2,166	1.09	0.84
19	44c	10/08/2011	513	859	96	374	81	26	94	15	88	490	18	54	8	48	7	2,773	1.35	0.72
20	45c	22/09/2011	437	769	86	345	73	23	82	13	74	413	15	44	6	40	6	2,426	1.28	0.76
21	46c	13/10/2011	402	699	78	308	65	20	70	11	64	353	13	38	5	35	5	2,167	1.30	0.79
22	47c	27/10/2011	455	790	89	346	73	23	82	13	73	411	15	45	6	41	6	2,469	1.30	0.77
23	48c	27/12/2011	367	656	75	297	63	19	64	10	57	300	11	33	5	29	4	1,991	1.24	0.86
24	49c	15/02/2012	383	709	84	343	74	23	79	12	67	349	14	39	6	36	6	2,222	1.16	0.82
25	50c	21/03/2012	363	699	84	343	74	22	76	11	62	334	13	37	5	35	5	2,162	1.10	0.84
26	51c	05/04/2012	391	740	89	359	78	23	80	12	69	357	14	39	6	36	6	2,300	1.12	0.83
27	52c	26/04/2012	384	719	86	348	75	23	77	12	68	349	14	39	5	36	5	2,241	1.13	0.82
28	53c	30/04/2012	388	719	86	349	76	23	78	12	66	349	14	38	6	36	6	2,246	1.14	0.83
29	54c	29/08/2012	396	729	87	357	78	23	79	12	69	356	14	40	6	36	6	2,287	1.15	0.82
30	55c	12/09/2012	384	705	84	340	74	22	75	12	65	338	13	38	5	34	5	2,196	1.15	0.83
31	56c	26/09/2012	384	723	87	353	77	23	81	12	67	348	14	39	6	36	6	2,255	1.11	0.82
32	57c	11/10/2012	399	746	89	360	80	24	81	12	68	351	14	39	6	36	6	2,309	1.14	0.85
33	58c	10/01/2013	351	641	77	312	67	20	66	10	55	281	11	31	4	29	4	1,959	1.16	0.90
34	59c	27/02/2013	420	744	89	361	77	23	77	12	65	327	13	37	5	34	5	2,290	1.20	0.89
35	60c	20/03/2013	385	707	84	345	75	22	74	11	61	311	13	35	5	33	5	2,166	1.16	0.89
36	61c	03/05/2013	374	707	86	351	78	23	78	12	66	341	14	38	5	35	5	2,215	1.10	0.84
37	62c	08/05/2013	390	730	87	358	79	23	77	12	64	328	13	37	5	35	5	2,243	1.13	0.88
38	63c	27/06/2013	376	708	85	349	75	22	73	11	61	312	13	36	5	33	5	2,164	1.12	0.88
39	64c	04/09/2014	340	662	81	331	73	22	71	11	59	295	12	33	5	30	5	2,028	1.07	0.89
40	65c	17/09/2014	305	594	73	299	66	20	64	10	53	264	11	30	4	26	4	1,824	1.06	0.89
41	66c	24/09/2014	324	638	78	322	70	21	68	10	55	280	11	32	4	28	4	1,946	1.05	0.91
42	67c	27/11/2014	326	596	74	302	66	20	64	10	52	259	10	29	4	25	4	1,841	1.12	0.94
43	68c	13/04/2015	249	502	63	260	58	17	56	8	46	229	9	26	4	23	4	1,552	1.00	0.89
44	69c	21/05/2015	275	535	67	278	61	18	59	9	49	240	10	27	4	25	4	1,660	1.03	0.90
45	70c	14/07/2015	209	421	53	223	49	15	47	7	39	192	8	22	3	20	3	1,311	0.99	0.91
46	71c	26/08/2015	167	353	45	191	43	13	43	6	36	174	7	20	3	18	3	1,120	0.95	0.86
47	72c	07/10/2015	146	305	39	164	37	11	35	5	29	141	6	16	2	14	2	951	0.95	0.90
48	73c	18/11/2015	157	330	42	177	40	12	39	6	32	156	6	18	2	16	2	1,034	0.94	0.88
49	74c	03/12/2015	186	392	50	209	47	14	45	7	36	179	7	20	3	18	3	1,215	0.94	0.90
50	75c	14/01/2016	189	398	51	210	47	14	45	7	36	179	7	21	3	18	3	1,227	0.95	0.91
51	76c	23/02/2016	169	359	46	192	44	13	41	6	34	167	7	19	3	16	2	1,118	0.93	0.91

TABLE 2. Rare Earth Elements concentrations (µg kg^{-1}). La/Pr and LREE/HREE ratios are normalized to the average volcanic local rock (Carr et al., 2013).

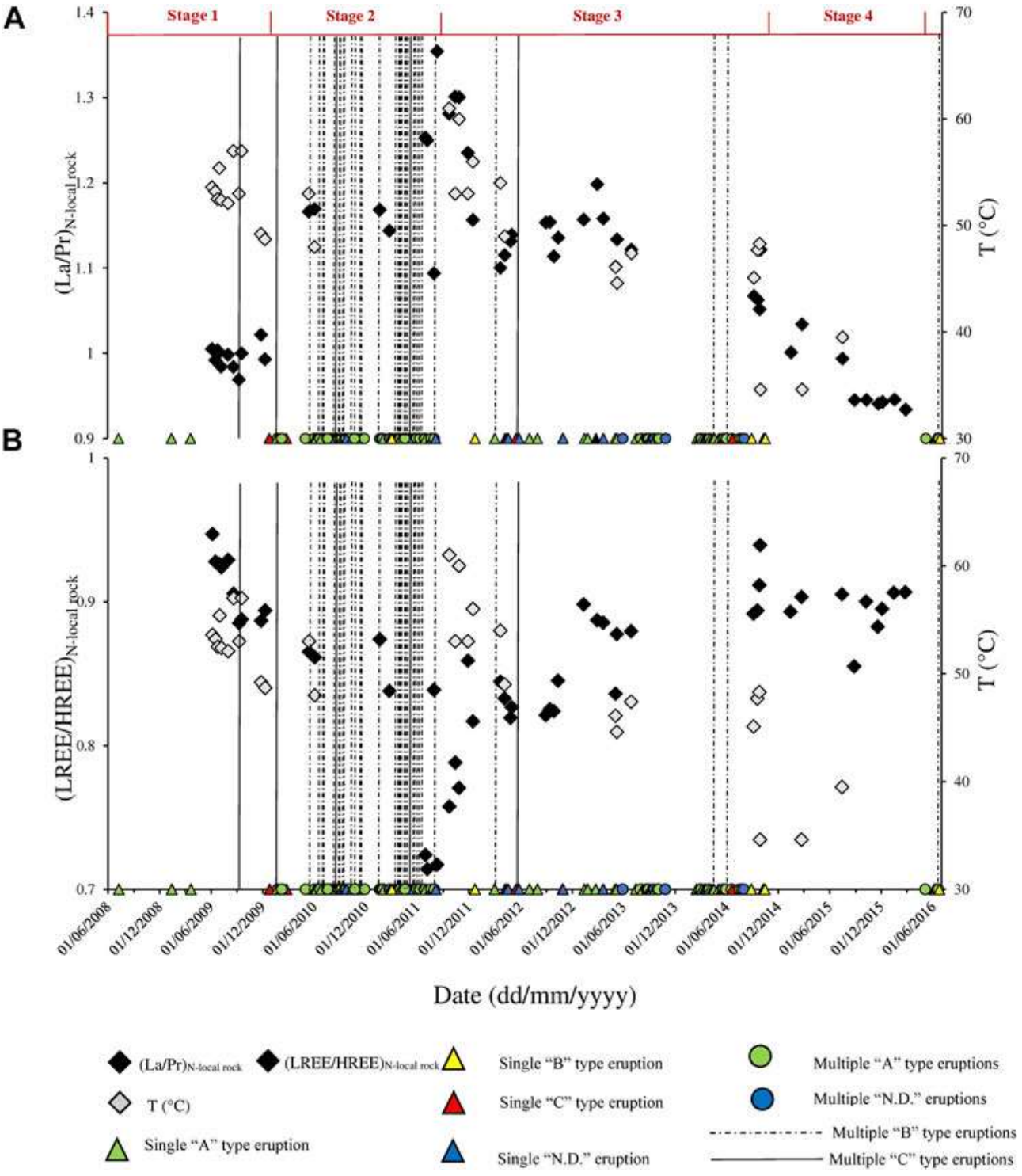

FIGURE 5. **(A)** $(La/Pr)_{N\text{-local rock}}$ and T vs. time. **(B)** $(LREE/HREE)_{N\text{-local rock}}$ and T vs. time.

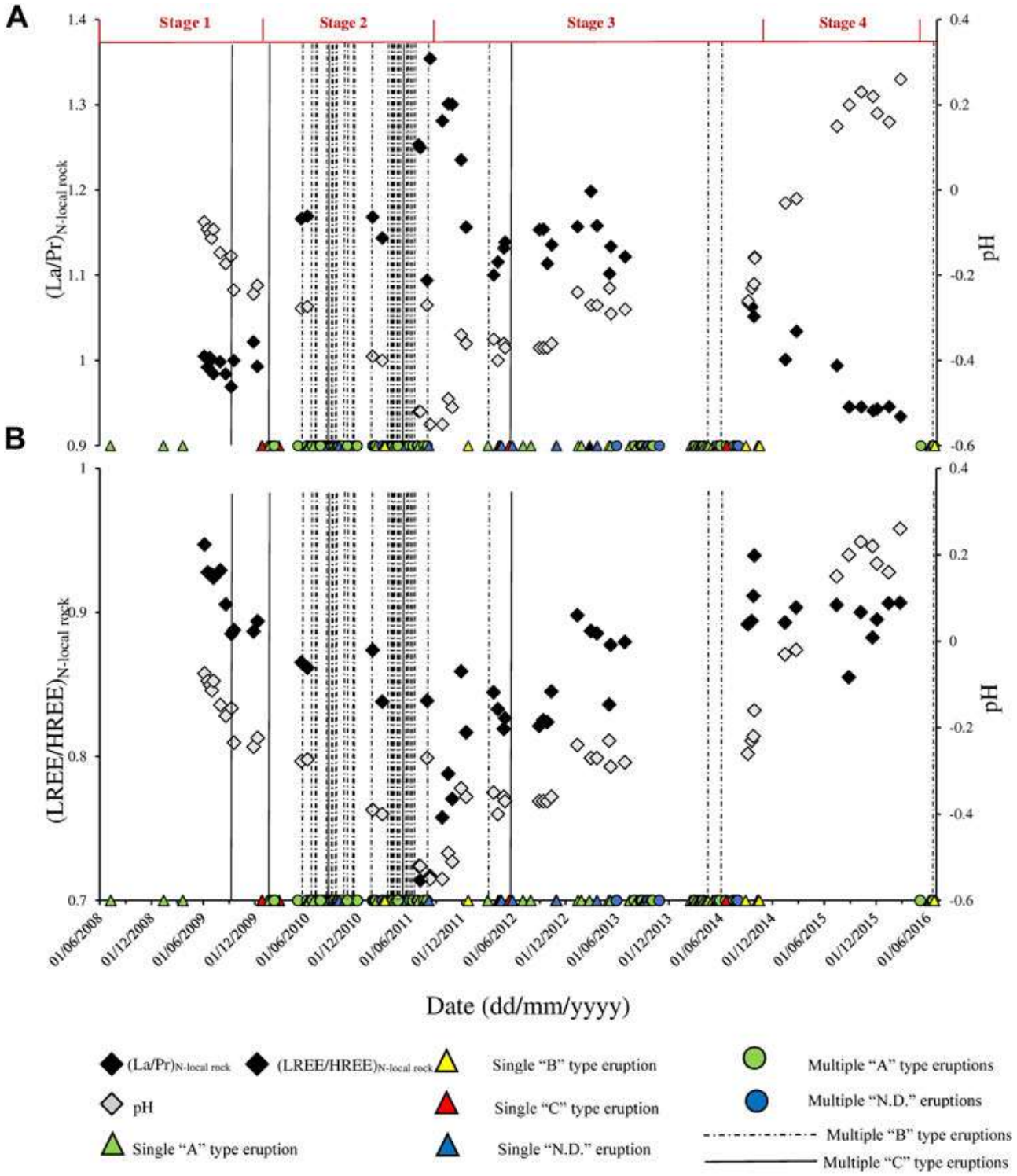

FIGURE 6. **(A)** $(La/Pr)_{N\text{-local rock}}$ and pH vs. time. **(B)** $(LREE/HREE)_{N\text{-local rock}}$ and pH vs. time.

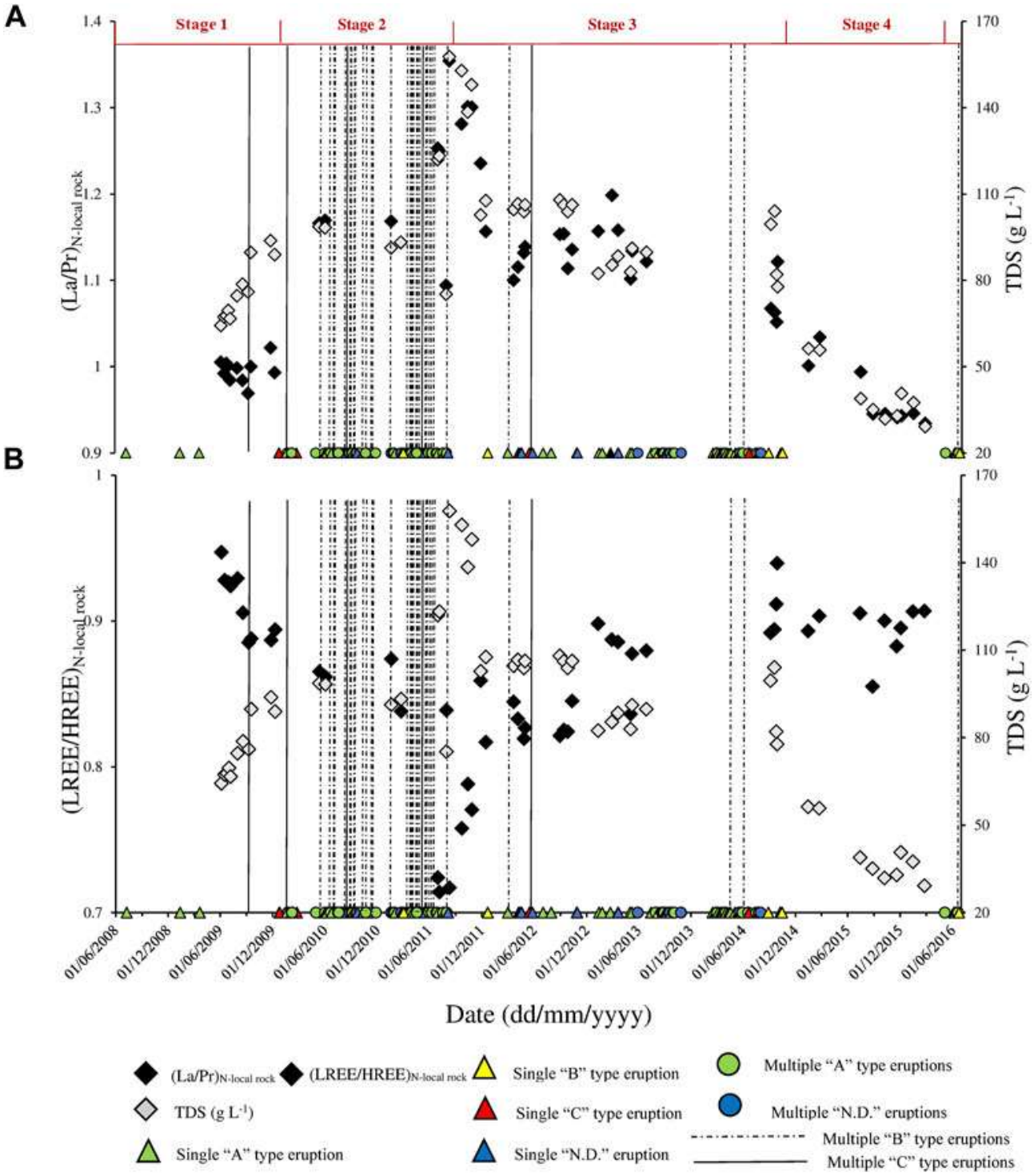

FIGURE 7. **(A)** $(La/Pr)_{N\text{-local rock}}$ and TDS vs. time. **(B)** $(LREE/HREE)_{N\text{-local rock}}$ and TDS vs. time.

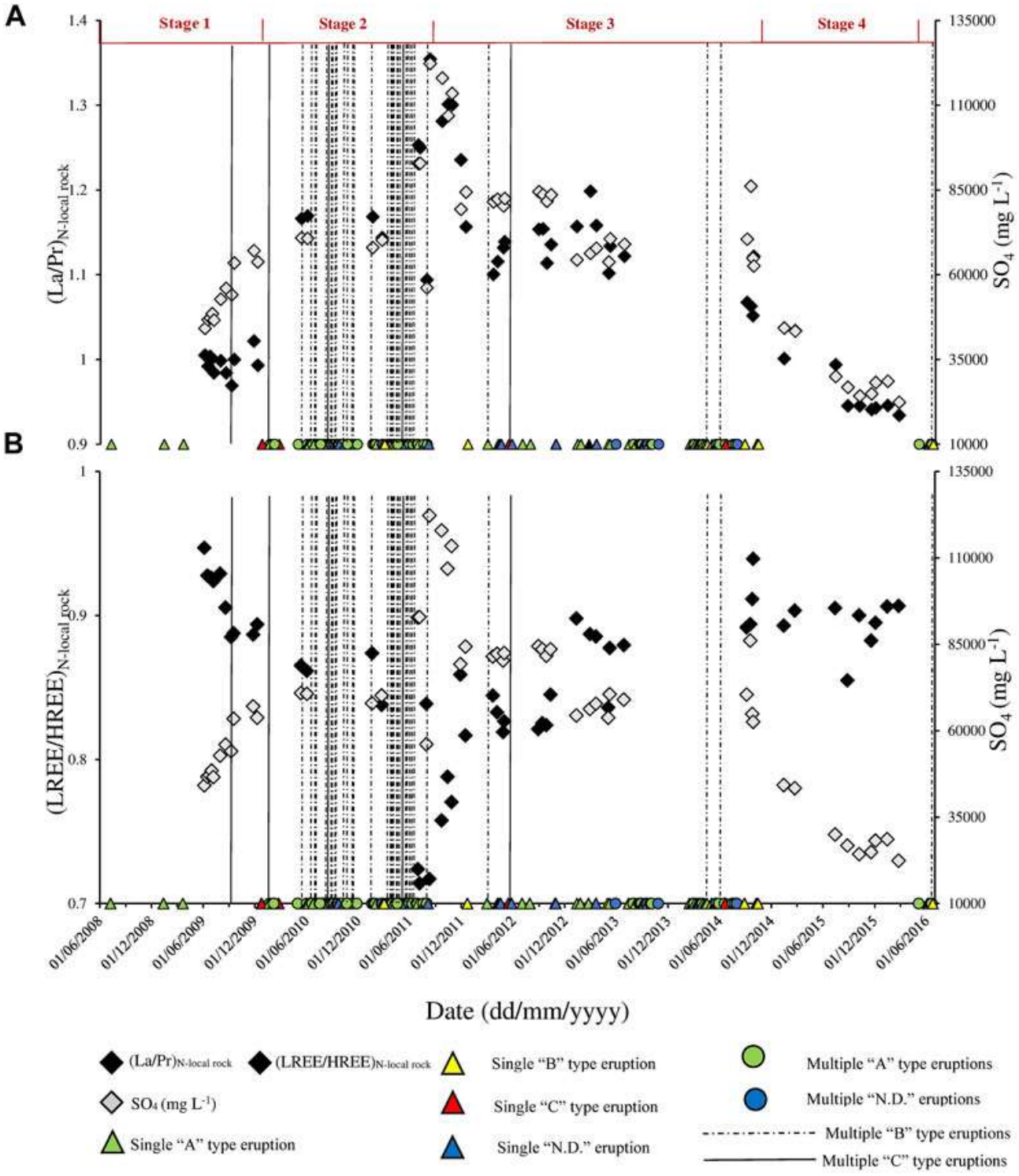

FIGURE 8. **(A)** $(La/Pr)_{N\text{-local rock}}$ and SO_4 vs. time. **(B)** $(LREE/HREE)_{N\text{-local rock}}$ and SO_4 vs. time.

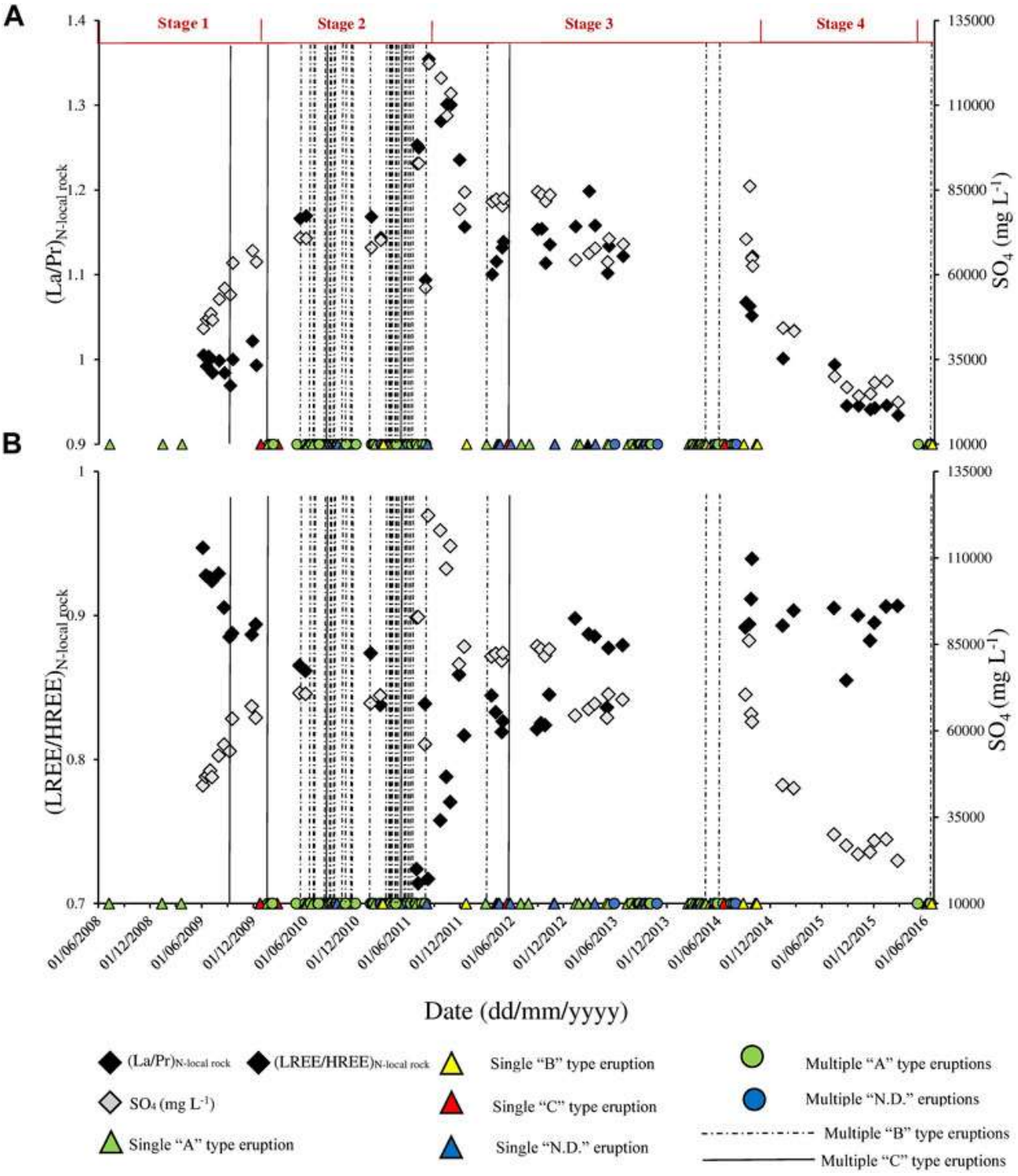

FIGURE 9. **(A)** $(La/Pr)_{N\text{-local rock}}$ and Ca vs. time. **(B)** $(LREE/HREE)_{N\text{-local rock}}$ and Ca vs. time.

The graph $(La/Pr)_{N\text{-local rock}}$ and temperature (T) versus time (Figure 5A) shows that the temperature of the lake water has a similar, though less marked trend, than the $(La/Pr)_{N\text{-local rock}}$ pattern. Unfortunately, the temperature data are not available for all the water samples. Instead, $(La/Pr)_{N\text{-local rock}}$ and pH versus time (Figure 6A) exhibit opposite trends, with pH decreasing when the volcanic activity increases. TDS and $(La/Pr)_{N\text{-local rock}}$ versus time (Figure 7A) and ΣREE and $(La/Pr)_{N\text{-local rock}}$ versus time (Figure 3A) show similar patterns from stages 1 to 4, with TDS, $(La/Pr)_{N\text{-local rock}}$, and ΣREE increasing with increasing phreatic activity. SO_4 concentrations vary identically to the $(La/Pr)_{N\text{-local rock}}$ pattern (Figure 8A). On the contrary, Ca concentrations decrease with increasing

$(La/Pr)_{N\text{-local rock}}$ and hence increasing phreatic activity (Figure 9A) and vice versa. The SO_4/Cl ratio (Supplementary Figure 2A) increases from 2008 to 2011, similar to the $(La/Pr)_{N\text{-local rock}}$ ratio. However, SO_4/Cl did not decrease back in 2016 with values similar to 2009, as recognized for all other described parameters. The Mg/Cl ratio (Supplementary Figure 3A) varies basically in the opposite way compared to $(La/Pr)_{N\text{-local rock}}$, decreasing during stage 2 of high-frequency activity.

As the $(LREE/HREE)_{N\text{-local rock}}$ ratio essentially behaves in the opposite way with respect to the $(La/Pr)_{N\text{-local rock}}$ ratio (i.e., decreasing when the phreatic activity increases and increasing when the phreatic activity decreases), this implies that the trends obtained comparing $(LREE/HREE)_{N\text{-local rock}}$ ratios with major element concentrations and their ratios, physico-chemical parameters of the waters, TDS and ΣREE values (Figures 3B, 5B–9B, Supplementary Figures 2B, 3B) are inverse to the ones obtained for $(La/Pr)_{N\text{-local rock}}$ ratio. The pattern of $(LREE/HREE)_{N\text{-local rock}}$ ratio shows a trend similar to the pH, Ca, and Mg/Cl patterns, while the trend is opposite with respect to the patterns of the remaining parameters and elements considered (T, TDS, ΣREE, SO_4, and SO_4/Cl).

The significance of the relation between all the variables was tested with a correlation matrix (Table 3). The result of the correlation coefficient calculated between two variables is a value between +1 and −1, where a correlation of +1 and a correlation of −1 show a perfectly positive and a perfectly negative correlation, respectively, while a correlation equal to 0 means that the relations between the two variables are not linear. The correlation coefficient calculated between $(La/Pr)_{N\text{-local rock}}$ and $(LREE/HREE)_{N\text{-local rock}}$ ratios is equal to −0.64, indicating a moderate negative correlation. The results in Table 3 show that the values of the correlation coefficient calculated for $(La/Pr)_{N\text{-local rock}}$ are in most cases higher with respect to the values of $(LREE/HREE)_{N\text{-local rock}}$ when they are compared to major elements, their ratios, and physico-chemical parameters. The pH, TDS, ΣREE, and SO_4 are the variables that are better correlated with $(La/Pr)_{N\text{-local rock}}$ and $(LREE/HREE)_{N\text{-local rock}}$ compared to the other parameters considered and display the highest values of the correlation coefficient, up to |0.90| for $(La/Pr)_{N\text{-local rock}}$. The absolute values of the correlation coefficients calculated between pH and $(La/Pr)_{N\text{-local rock}}$ and between pH and $(LREE/HREE)_{N\text{-local rock}}$ are higher than the correlation coefficients calculated for the temperature; however, the incompleteness of the temperature data set makes it difficult to compare them. For comparison, we also report the correlation coefficients of various major elements that are not presented in the graphs (Figures 3, 5–9; Na, K, Mg, Al, Fe, and Cl). All the major elements considered show a positive value of the correlation coefficient when compared to $(La/Pr)_{N\text{-local rock}}$, except Ca, which is the only major element with a negative value of the correlation coefficient. On the contrary, Ca is the only positively correlated to $(LREE/HREE)_{N\text{-local rock}}$. Furthermore, the correlation coefficient of all the major elements (except Ca) with TDS is positive, with values that span from 0.69 to 0.99. Ca is the only major element that exhibits a negative value of the coefficient when compared to TDS, the only one with a correlation value < |0.50|. Mg/Cl ratio displays higher values of the correlation coefficient for both $(La/Pr)_{N\text{-local rock}}$ and $(LREE/HREE)_{N\text{-local rock}}$ relations compared to SO_4/Cl ratio. The latter is also the variable with the lowest correlation coefficients calculated.

	La/Pr	LREE/HREE	T	pH	TDS	ΣREE	Na	K	Mg	Al	Fe	Ca	SO_4	Cl	SO_4/Cl	Mg/Cl
La/Pr	1															
LREE/HREE	−0.64	1														
T	0.21	−0.48	1													
pH	−0.87	0.54	−0.49	1												
TDS	0.88	−0.62	0.49	−0.96	1											
ΣREE	0.81	−0.52	0.37	−0.94	0.88	1										
Na	0.67	−0.70	0.68	−0.73	0.69	0.67	1									
K	0.86	−0.67	0.54	−0.92	0.91	0.85	0.71	1								
Mg	0.59	−0.47	0.70	−0.75	0.73	0.71	0.71	0.67	1							
Al	0.83	−0.62	0.59	−0.93	0.94	0.85	0.73	0.91	0.81	1						
Fe	0.66	−0.58	0.58	−0.73	0.70	0.68	0.93	0.68	0.67	0.76	1					
Ca	−0.62	0.67	0.06	0.40	−0.45	−0.41	−0.40	−0.49	−0.05	−0.40	−0.38	1				
SO_4	0.90	−0.62	0.42	0.95	0.99	0.87	0.66	0.91	0.68	0.92	0.68	−0.49	1			
Cl	0.76	−0.55	0.64	−0.90	0.93	0.83	0.69	0.82	0.85	0.90	0.70	−0.28	0.89	1		
SO_4/Cl	0.18	−0.07	−0.45	0.01	0.02	−0.01	−0.16	0.03	−0.46	−0.10	−0.14	−0.43	0.12	−0.33	1	
Mg/Cl	−0.53	0.23	−0.19	0.62	−0.65	−0.54	−0.23	−0.56	−0.14	−0.51	−0.32	0.38	−0.66	−0.59	−0.03	1

TABLE 3. Correlation matrix.

5 Discussion

5.1 Temporal Variations in Major Elements, REE, and Physico-Chemical Parameters

The first interesting result from our dataset is that the behavior of REE, especially $(La/Pr)_{N\text{-local rock}}$ and $(LREE/HREE)_{N\text{-local rock}}$ ratios, varies with time following the main variations of volcanic activity, represented by the occurrence of hundreds of phreatic eruptions (679). Despite the impossibility of identifying an unequivocal cause-effect relation between $(La/Pr)_{N\text{-local rock}}$ and $(LREE/HREE)_{N\text{-local rock}}$ ratios variations with the occurrence of a single phreatic eruption, the general trend of both ratios seems to be related to the frequency of phreatic eruptions, here expressed in stages 1 to 4 throughout 2008–2016. Consequently, it is not possible to discern how the different types of eruptions (A, B, and C) affected the trend of $(La/Pr)_{N\text{-local rock}}$ and $(LREE/HREE)_{N\text{-local rock}}$ ratios over time.

Rouwet et al. (2017, 2019) describe in detail how physico-chemical parameters, concentrations of major elements, and major element ratios vary at Laguna Caliente for the period 2005–2010 and 1978–2016, respectively. They suggest that pH is one of the most effective parameters to detect changes in volcanic activity, indicative of the general degassing state of the volcano caused by SO_2, H_2S, HCl, and HF input. They did not deem an increased temperature a strong indicator for enhanced phreatic activity, as, on the contrary, a temperature decrease is often an indication of conduit sealing, causing pressure build-up beneath a lake before phreatic eruptions.

Rouwet et al. (2019) also found that concentrations of $SO_4 > 60{,}000$ mg L^{-1} are associated with the most intense eruptive phases (e.g., stage 2, 2010–2011), while SO_4/Cl does not work as a strong indicator, probably because of the loss of HCl by evaporative degassing (Capaccioni et al., 2017; Rouwet et al., 2017). Supplementary Figures 2A,B display that the SO_4/Cl ratio steadily increases from 2012 to 2016 despite the number of phreatic eruptions in decline. This trend coincides with the steady lake level drop throughout the entire 2006–2016 phreatic eruption cycle, eventually leading to full lake dry out in 2017. The smaller Laguna Caliente becomes hence more sensitive to HCl degassing through time, imposing inertia on the parameter SO_4/Cl, making it less sensitive and adapted for monitoring purposes (Rouwet et al., 2017).

Since pH and SO_4 seem to represent the most sensitive parameters to monitor the volcanic activity at Laguna Caliente during the eruptive cycle of 2006–2016 (Rouwet et al., 2017; Rouwet et al., 2019), their strong correlation with $(La/Pr)_{N\text{-local rock}}$ and the correlation with $(LREE/HREE)_{N\text{-local rock}}$ (even if

lower compared with $(La/Pr)_{N\text{-local rock}}$ ratio) suggest that they are good indicators of changes in volcanic activity, especially the case for $(La/Pr)_{N\text{-local rock}}$ (Table 3; Figures 6, 8).

Comparing the variations of Na, K, Mg, Ca, Al, and Fe with the volcanic activity over time, we notice that the concentrations of all the major elements, except Ca, rise when the frequency of the eruptions is higher and decline consequently with a lower frequency of phreatic eruptions. The opposite behavior of Ca compared with the other cations can be explained by secondary processes such as the precipitation of gypsum/anhydrite at the surface of the lake or at depth (Rouwet et al., 2017; Inguaggiato et al., 2018 and references therein). The loss of cations at Laguna Caliente mainly depends, in fact, on minerals precipitation (Rouwet et al., 2019). Since TDS is representative of the variations of all the major elements, except Ca, only the latter was compared with $(La/Pr)_{N\text{-local rock}}$ and $(LREE/HREE)_{N\text{-local rock}}$ ratios (Figures 9A,B).

Trends in major elements and physico-chemical parameters suggest that the increase in phreatic activity is related to a higher input of volcanic gases (SO_2, HCl, and HF), in agreement with the gas-driven mechanism of phreatic eruptions (de Moor et al., 2016; Stix and de Moor, 2018). The pH values decrease consequently when gas input is higher. A lower pH renders the water more aggressive during water-rock interaction and hence favors the leaching of rock-forming elements (i.e., cations), resulting in higher TDS values. Despite the greater leaching of rock-derived elements, the opposite trend of Ca is probably due to the gypsum/anhydrite precipitation, a process that mainly affects Ca concentration over time.

Considering the high amount of SO_4 (2–3 orders of magnitude higher with respect to Ca due to massive SO_2 input), the precipitation of gypsum/anhydrite did not induce significant variations in the SO_4 temporal pattern. This could be explained regarding the abundance of SO_4 compared to Ca, which represents, in fact, the limiting reagent for the gypsum/anhydrite precipitation process.

The fact that REE concentrations, as well as changes of $(La/Pr)_{N\text{-local rock}}$ and $(LREE/HREE)_{N\text{-local rock}}$ ratios in the water of Laguna Caliente, are related to the variations of the volcanic activity suggests that REE chemistry could provide additional information on changes in activity and fluid-mineral dynamics to the "classical" monitoring parameters (major elements and their ratios, physico-chemical parameters). Moreover, the variations of $(La/Pr)_{N\text{-local rock}}$ and $(LREE/HREE)_{N\text{-local rock}}$ ratios with varying activity have often revealed a higher sensitivity than, e.g., T and SO_4/Cl ratios.

5.2 Rock Dissolution, Precipitation of Secondary Minerals, and REE Fractionation

Several authors presented that solubility of anhydrite and alunite is retrograde (Bernard et al., 2004; Taran et al., 2008; Colvin et al., 2013; Kalacheva et al., 2015). Rodríguez and van Bergen (2017) ran thermodynamic simulations with PHREEQC to investigate the saturation indexes of representative minerals from lake surface temperature up to 300°C. They show that the solubility of gypsum, anhydrite, and alunite decreases when the temperature increases. In particular, the solubility curve of gypsum is prograde from 0 to ~40°C and retrograde for temperature higher than ~40°C and intercepts the solubility curve of anhydrite at a temperature of ~40°C (Azimi et al., 2010). The increase of the temperature in a volcanic hydrothermal system can hence induce the precipitation of secondary minerals: 1) at the surface when the temperature increases due to the changes of the volcanic activity or 2) in the deeper and hotter part of the system. The processes of precipitation and dissolution of secondary minerals do not only affect the mobility of the main elements that constitute the minerals but also other solutes, including REE. Data from previous studies have demonstrated that minerals such as alunite and gypsum can fractionate the REE in hyperacid fluids (Varekamp, 2015; Inguaggiato et al., 2017; van Hinsberg et al., 2017; Inguaggiato et al., 2018; Inguaggiato et al., 2020a; Inguaggiato et al., 2020b; van Hinsberg et al., 2020).

The isosol plot was used here to calculate the grams of rock dissolved per liter of solution, considering the congruent dissolution of the average local rock (andesite), consequently to the water-rock interaction process (Varekamp, 2015). The average chemical composition of major elements in the local andesite for Poás was provided by Cigolini et al. (1991). The amount of local rock dissolved was estimated graphically for all the water samples and varies between ~10 and ~70 g per liter of water; our attention is mainly focused on Ca, Al, K, and Na depletion (constituents of gypsum, anhydrite, and alunite) compared to the hypothetical congruent dissolution of the local rock. Four isosol plots, one for each stage of volcanic activity, were selected as representative of the variation of the dissolution of the local rock and the precipitation of secondary minerals during the activity changes (Figures 10A–D). During stage 1 (Figure 10A; low phreatic activity), almost all the elements considered lie on the 25 g rock/L line, indicating that gypsum/anhydrite, as well as alunite, could not precipitate in high amounts. At stage 2 (Figure 10B; high phreatic activity), the increase of rock dissolution occurs during the increase of temperature and the decrease of the pH of the lake, leading to the highest amount of rock dissolved. Considering the congruent dissolution of the local rock, Ca concentration is strongly depleted with respect to the Ca that should be dissolved in lake water. Aluminum, Na, and K plots on the line are representatives of the congruent dissolution of the rock (50 g rock/L). The precipitation of minerals containing Ca (such as gypsum/anhydrite) is proposed to justify the Ca depletion. During stage 3 (Figure 10C; the decline of phreatic activity), the amount of rock dissolved (~35 g rock/L) and the loss of Ca dissolved (gypsum/anhydrite precipitation) are both lower with respect to those of stage 2. Once more, Al, Na, and K are not depleted. Rock dissolution representative of stage 4 (Figure 10D; quiescent period) is ~17 g rock/L, with Ca and Al concentrations in lake water comparable to that of the congruent rock dissolution line. These findings confirm that the water-rock interaction processes have varied between 2009 and 2016.

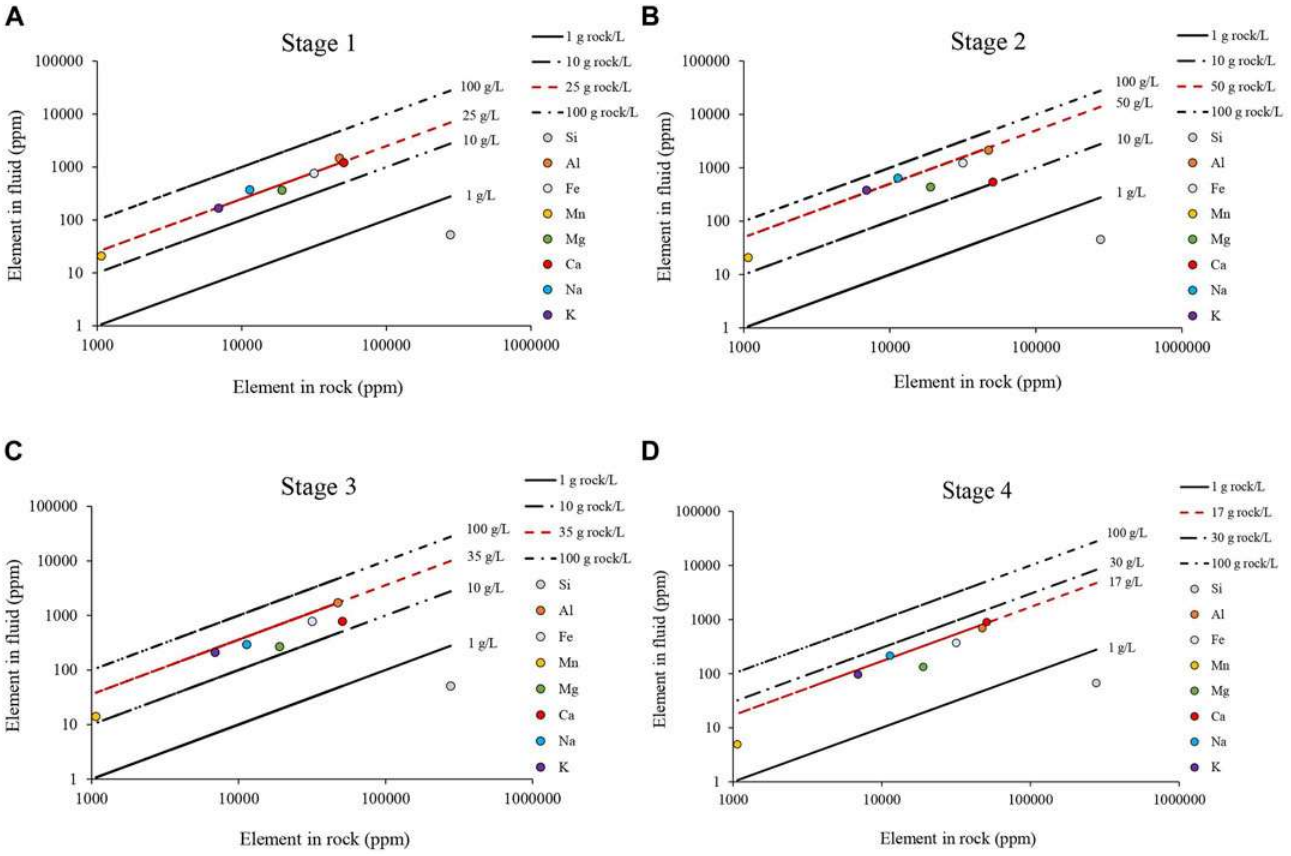

FIGURE 10. Isosol plots show that the amount of rock dissolved per liter of lake water and the loss of elements in water, especially Ca loss, is considered the effect of the gypsum/anhydrite

precipitation. The four isosol plots are representative of the dissolution of the rock and the Ca loss during **(A)** stage 1, **(B)** stage 2, **(C)** stage 3, and **(D)** stage 4.

Rock dissolution is favored by more acidic waters, especially evident for the peak activity stages 2 and 3. Contrarily, rock dissolution is less intense during stage 1 (very few phreatic eruptions) and stage 4 (no evidence of phreatic activity) (Supplementary Figure 4).

The estimation of the amount of congruent dissolution of g rock per liter allowed calculating the element loss (element*; ppm) for all the water samples, using the following equation:

$$element^{*}=element_{(isosol)}-element_{(analyzed)}, \quad (1)$$

where $element_{(isosol)}$ represents the concentration of the element in the lake water (ppm) resulting from the congruent dissolution of the rock calculated with the isosol plot, while $element_{(analyzed)}$ is the concentration of the elements (ppm) effectively measured in the lake water. The loss of Ca, Al, K, and Na (Ca*, Al*, K*, Na*) was calculated to consider the potential precipitation of sulfate minerals. The loss of Ca can be the consequence of gypsum ($CaSO_4{*}2H_2O$) and/or anhydrite ($CaSO_4$) precipitation; the loss of Al, Na, and K can be due to the precipitation of alunite minerals [$(Na, K)Al_3(SO_4)_2(OH)_6$] (Colvin et al., 2013; Varekamp, 2015). The results of Ca*, Al*, K*, and Na* were plotted vs. $(La/Pr)_{N\text{-local rock}}$ and $(LREE/HREE)_{N\text{-local rock}}$ ratios, respectively (Figures 11A–H). Near-linear trends can be observed for $(La/Pr)_{N\text{-local rock}}$ vs. Ca* and $(LREE/HREE)_{N\text{-local rock}}$ vs. Ca* (Figures 11A,B): increasing the loss of Ca interpreted as gypsum/anhydrite precipitation, the $(La/Pr)_{N\text{-local rock}}$ increases and $(LREE/HREE)_{N\text{-local rock}}$ decreases. These observations corroborate 1) the distribution coefficients calculated during the precipitation of gypsum from the hyperacid and hypersaline waters of Kawah Ijen and Laguna Caliente crater lakes (Inguaggiato et al., 2018; Inguaggiato et al., 2020a), 2) the REE pattern of gypsum collected from the Kawah Ijen terrace, with the seeped-out crater lake water as source fluid (van Hinsberg et al., 2017), and 3) the REE patterns of gypsum precipitated in the laboratory from a synthetic solution (Dutrizac, 2017). The lack of trends of $(La/Pr)_{N\text{-local rock}}$ and $(LREE/HREE)_{N\text{-local rock}}$ each one versus Al*, Na*, and K* (Figures 11C–H) allows suggesting that the precipitation of alunite, as well as other Al-bearing minerals, is not the main process fractionating the REE over time.

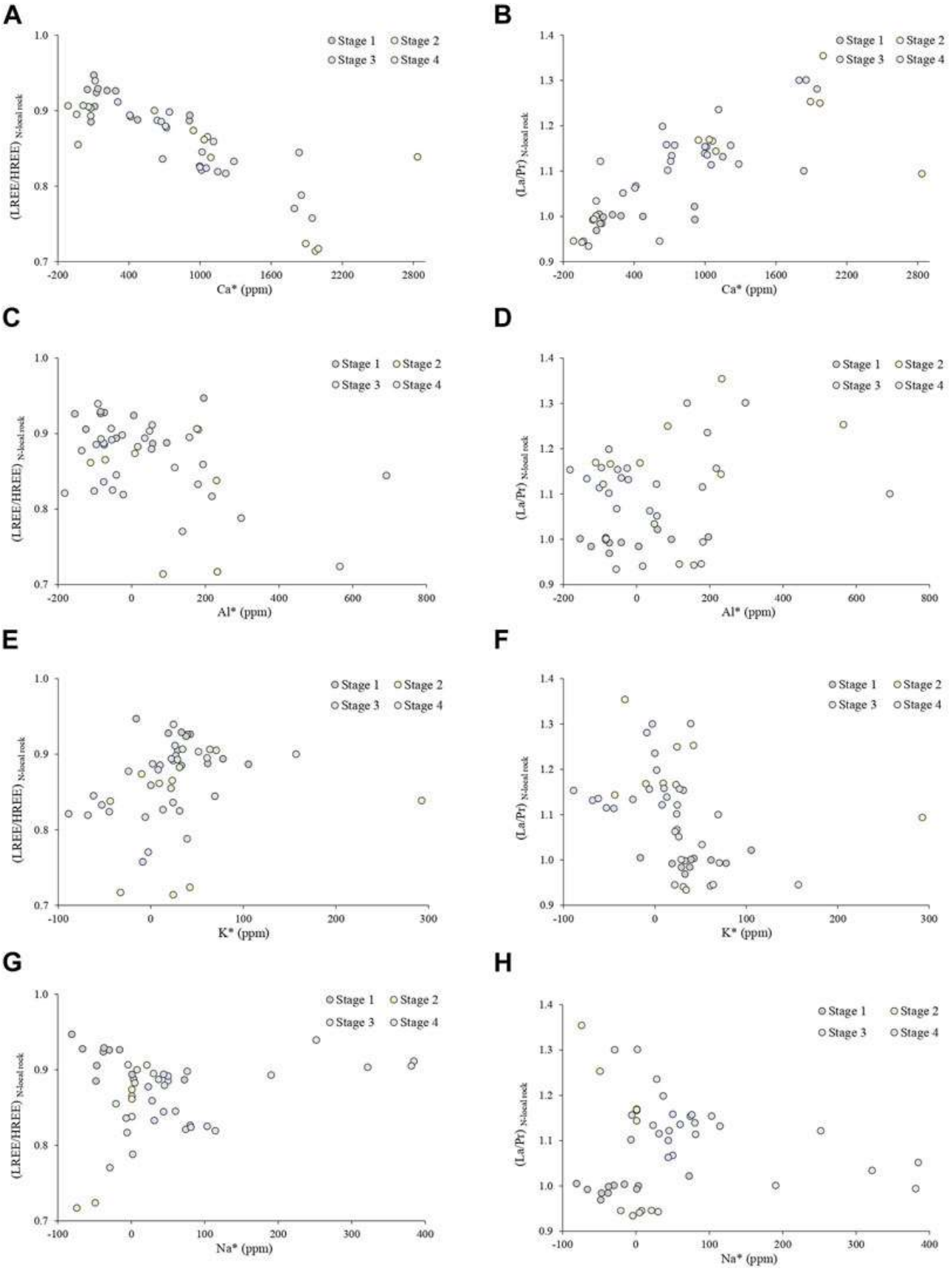

FIGURE 11. **(A)** Ca* in lake water vs. $(LREE/HREE)_{N\text{-local rock}}$. **(B)** Ca* in lake water vs. $(La/Pr)_{N\text{-local rock}}$. **(C)** Al* in lake water vs. $(LREE/HREE)_{N\text{-local rock}}$. **(D)** Al* in lake water vs. $(La/Pr)_{N\text{-local rock}}$. **(E)** K* in lake water vs. $(LREE/HREE)_{N\text{-local rock}}$. **(F)** K* in lake water vs. $(La/Pr)_{N\text{-local rock}}$. **(G)** Na* in lake water vs. $(LREE/HREE)_{N\text{-local rock}}$. **(H)** Na* in lake water vs. $(La/Pr)_{N\text{-local rock}}$.

5.3 Processes Affecting REE Fractionation and Their Implications Over Time

Previous studies have already focused on comparing REE variations over time in volcanic fluids and their possible connection with volcanic unrest. Wood (2006) analyzed the patterns of REE in the crater lake of Mount Ruapehu (New Zealand) between 1993 and 1998, a period including the 1995–1996 phreatomagmatic eruption. The REE chondrite normalized patterns vary over time, specifically before and after the eruption occurred in September 1995. The author suggests that the concentrations of REE in the crater lake could probably be correlated with the variation of the volcanic activity. Varekamp (2015), comparing the REE concentrations in the thermal spring fluids of Copahue volcano (Argentina-Chile), found that the La/Sm ratio varied over time (1997–2005), with a minimum in 2000, concomitant with an eruption. REE patterns in the hyperacidic crater lake water of Santa Ana volcano (El Salvador) during 2017 show changes in the LREE/HREE normalized ratios (Colvin et al., 2013). The depletion of LREE was considered as the effect of alunite precipitation (Varekamp, 2015). Morton-Bermea et al. (2010) did not notice an important correlation between REE variations and volcanic activity at El Chichón volcano (Mexico), probably due to the relative stability of the volcanic activity during the period of observation and the less extreme pH (H_2S dominated degassing) and salinity of its crater lake (Rouwet et al., 2008).

Inguaggiato et al. (2018) investigated the REE fractionation during the in-lab precipitation of gypsum from the Laguna Caliente lake waters and proposed that the pattern of REE in water is also controlled by the precipitation of gypsum, a process that naturally occurs at the crater lake (Brantley et al., 1987). They pointed out that gypsum preferentially incorporates LREE with respect to HREE, affecting the relative proportion between the two sub-groups, as also described in detail in Section 4.2. Moreover, Ce, Pr, and Nd distribution coefficients, calculated between gypsum and the lake waters of Poás and Kawah Ijen volcanoes, are higher compared with the other REE, including La that is part of the LREE (Inguaggiato et al., 2018; Inguaggiato et al., 2020a). Hence, the preferential incorporation of LREE in gypsum, particularly Pr, is also corroborated by 1) the opposite trend of Ca concentration with respect to $(La/Pr)_{N\text{-local rock}}$ ratio and 2) the same trend of Ca with respect to $(LREE/HREE)_{N\text{-local rock}}$ ratio in this study.

The maximum value of Ca* calculated (2,835 ppm) corresponds to the precipitation of 12 g of gypsum per kg of water. Higher loss of Ca was calculated in lake waters of stages 2 and 3 (periods of high volcanic activity), interpreted as a higher amount of gypsum/anhydrite precipitated than that in stages 1 and 4. A mass balance was simulated to remove REE from lake water during the precipitation of gypsum in a range from 2 to 12 g of gypsum per kg of water. The average REE concentrations of the water samples belonging to stage 1 (low volcanic activity), with $(La/Pr)_{N\text{-local rock}}$ and $(LREE/HREE)_{N\text{-local rock}}$ values close to 1, were considered as the initial point when the REE ratios are not affected by strong fractionation processes. The concentration of each REE in gypsum ($[REE_i]_{gypsum}$) precipitated from the lake was calculated using the concentration of each REE in the water before considered as initial point $[REE_i]_{water}$, and the average distribution coefficients of each REE (K_D) in the gypsum precipitated in the laboratory from Laguna Caliente lake water (Inguaggiato et al., 2018):

$$[REE_i]_{gypsum} = [REE_i]_{water} * K_D . (2)$$

Once the REE concentrations in the gypsum were known, REE concentrations for different amounts of gypsum precipitated per kg of water (six steps: 2, 4, 6, 8, 10, and 12 g of gypsum) were calculated and then subtracted from the REE concentrations of the initial lake water considered $[REE_i]_{water}$. The results mainly show an increase of the $(La/Pr)_{N\text{-local rock}}$ ratio (1–1.12) and a decrease of the $(LREE/HREE)_{N\text{-local rock}}$ ratio (0.92–0.77). The REE ratios of the lake water, calculated during the simulation of gypsum precipitation, are in the range of values found in the lake water over time;

$(La/Pr)_{N\text{-local rock}}$ ratio ranges from 0.93 to 1.35 and $(LREE/HREE)_{N\text{-local rock}}$ ratio ranges 0.71–0.95. The highest depletion of LREE is associated with the precipitation of 12 g of gypsum per kg of water (Figure 12), corresponding to the loss of Ca estimated in one of the water samples belonging to stage 2. These results allow proposing that the amount of gypsum precipitated is adequate to justify the changes of $(LREE/HREE)_{N\text{-local rock}}$ ratios over time.

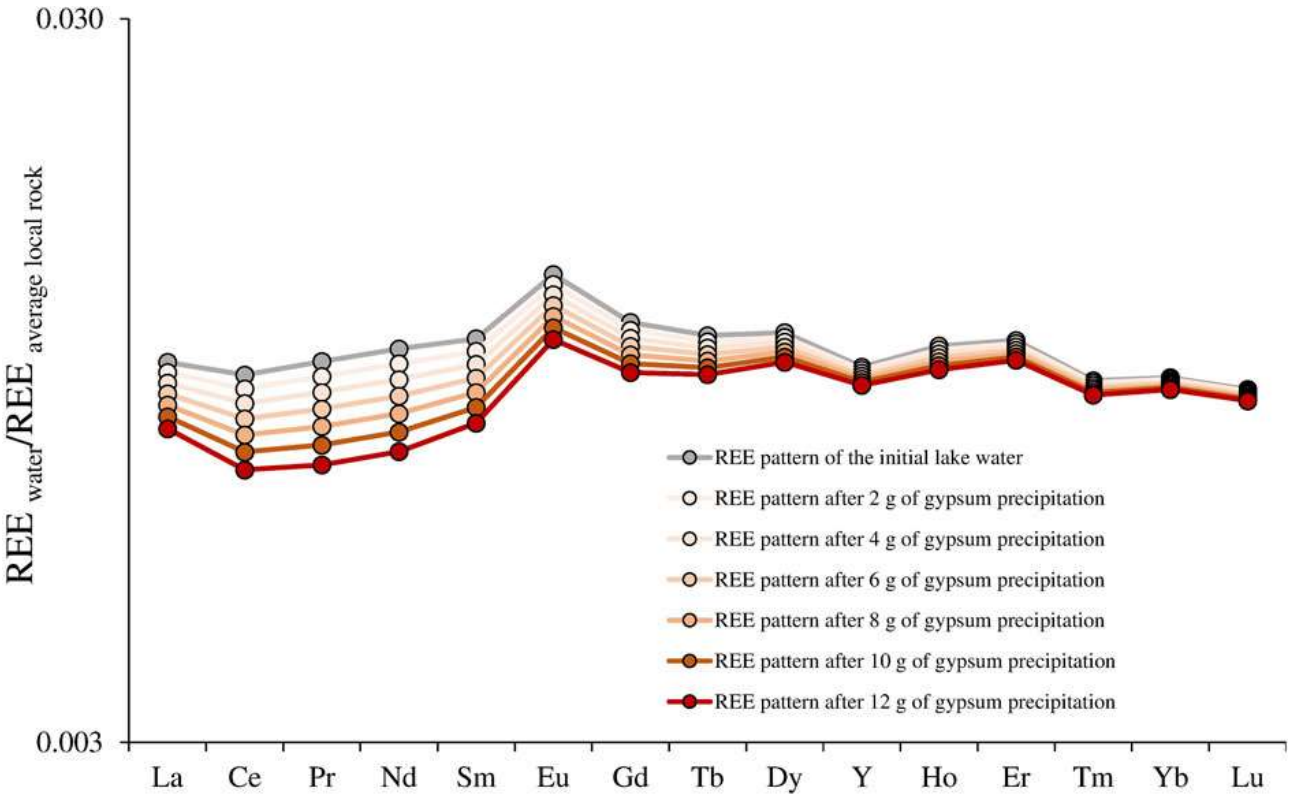

FIGURE 12. REE concentrations in lake water normalized to the average local rock (Carr et al., 2013) after 2, 4, 6, 8, 10, and 12 g of gypsum precipitation. The average REE concentration [REEi]water was used as the initial point and calculated considering the samples of stage 1 characterized by $(La/Pr)_{N\text{-local rock}}$ and $(LREE/HREE)_{N\text{-local rock}}$ ratios close to 1. REE concentrations removed from the gypsum precipitation were subtracted to the [REEi] water and plotted.

Martínez (2008) studied the variations of REE at the crater lake and thermal springs at Poás volcano during the period 1978–2007 and found that the concentrations of REE vary over time; specifically, some REE patterns show a depletion of LREE, as also shown in this investigation. The author suggests that the depleted LREE patterns could result from 1) fluid interaction with altered rocks that were already depleted in LREE or 2) LREE incorporation in alunite. Taking into consideration that REE patterns of alunite group minerals in other volcanic hydrothermal systems (Kikawada et al., 2004) are also enriched in LREE, it is likely that the precipitation of alunite in Laguna Caliente crater lake could also favor the decrease of $(LREE/HREE)_{N\text{-local rock}}$ in the water. However, both $(La/Pr)_{N\text{-local rock}}$ and $(LREE/HREE)_{N\text{-local rock}}$ ratios show trends only with Ca*, in contrast to Al*, K*, and Na*. Furthermore, the higher loss of Ca (Ca*) with respect to the loss of Al (Al*) indicates that the amount of gypsum/anhydrite precipitated is greater than the quantity of alunite precipitated. These findings confirm that gypsum and/or anhydrite precipitation play an important role in fractionating the REE in the hyperacid crater lake of Laguna Caliente over time. Moreover, Martinez (2008) also identified gypsum in lake bottom sediments and suspended particulate in the lake water column. The findings of gypsum in lake water corroborate that the Ca loss can be justified by gypsum or anhydrite precipitation. We cannot exclude the precipitation of alunite in the Poás volcanic hydrothermal system and the participation of the alunite in the REE fractionation in water.

The low pH values of the lake waters registered from 2008 to 2016, during the increase of the volcanic activity, reflect an enhanced input of acidic gases (such as SO_2, HCl, and HF), causing highly effective leaching of REE and major elements from "fresh" volcanic rock, probably also accentuated by continuous lake evaporation. This is consistent with the increasing concentrations of ΣREE over time concurrently to an enhanced gas input and the related pH drop. The rise of $(La/Pr)_{N\text{-local rock}}$ ratio and the decrease of $(LREE/HREE)_{N\text{-local rock}}$ ratio, when phreatic activity is more intense, are consistent with the possible gypsum/anhydrite precipitation that affects the concentrations of REE incorporating LREE preferentially with respect to HREE and Pr with respect to La.

Based on the highest Mg/Cl ratios before the 2006–2016 phreatic eruption cycle, Rouwet et al. (2017) argued that the resumed phreatic unrest was caused by the intrusion of a new magma batch in 2005 or before, also supported by geophysical (gravity, Rymer et al., 2009) and gas geochemical surveys (Vaselli et al., 2003; Fischer et al., 2015). These findings highlight that the variations of REE at Laguna Caliente during the period 2009–2016, as well as the common parameters used in volcano monitoring here reported for comparison, are connected to the occurrence of volcanic activity changes observable at the surface as multiple eruptions.

6 Conclusion

The crater lake of Poás volcano, Laguna Caliente, was sampled between June 2009 and February 2016, the period concerning the phreatic eruption cycle before the April 2017 phreatomagmatic eruption. The occurrence of hundreds of phreatic eruptions at Laguna Caliente during our sampling period provided a unique occasion to study the role of REE as possible indicators for volcano monitoring at active hyperacid crater lakes.

The concentrations of REE dissolved in the lake water vary from 950 to 2,773 μg kg^{-1}, increasing as the phreatic activity increases. The temporal evolution of $(La/Pr)_{N\text{-local rock}}$ and $(LREE/HREE)_{N\text{-local rock}}$ ratios shows a clear relation with changes in volcanic activity, i.e., increasing and decreasing, respectively, when the frequency of phreatic eruptions is higher. The similarities observed comparing the patterns of $(La/Pr)_{N\text{-local rock}}$ and $(LREE/HREE)_{N\text{-local rock}}$ ratios with those of physico-chemical parameters, major elements concentrations, and major elements ratios, "classically" used for volcanic lakes surveillance suggest that their variations seem to occur concurrently. The isosol plot, used to calculate the g of rock per liter of lake water dissolved during the congruent dissolution over time (10–70 g/L), shows that the highest values were found in stage 2. The opposite behavior of Ca with respect to the other major elements suggests an important depletion of this element in the water caused by Ca-bearing mineral precipitation, like gypsum and/or anhydrite. The different amount of Ca loss in the water during the four stages of volcanic activity indicates that the precipitation process is greater during the stages of high phreatic activity. Mass balance calculation confirms that the gypsum precipitation, estimated during the period of observation, is a good candidate to justify the depletion of LREE observed in the REE patterns in lake water. Our observations on REE changes over time and their relations with the changes of major elements, physico-chemical parameters, and the major changes of the volcanic activity between 2009 and 2016 at Laguna Caliente demonstrate that REE chemistry is an interesting tool in order to study water-rock interaction processes at Poás volcano, or elsewhere. However, further studies on the usefulness of REE in Laguna Caliente crater lake and in other hyperacid crater lakes are required to generalize the findings of this investigation about the connection of REE with volcanic monitoring.

Data Availability Statement

The original contributions presented in the study are included in the article/Supplementary Material; further inquiries can be directed to the corresponding author.

Author Contributions

SP wrote the original draft of the manuscript and elaborated the dataset. CI and SP formulated the scientific question, designed the study, and the scientific approach. CI and DR edited the first draft of the manuscript by writing part of the sections. RM-A, CR-U, GG, and DR organized and performed the field sampling. LP and GL revised and edited a version of the manuscript and added new ideas. LB and SB performed the analysis in laboratory. All authors contributed to the final version of the manuscript.

Funding

This work was partially supported by the Istituto Nazionale di Geofisica e Vulcanologia (INGV; Italy), Centro de Investigación Científica y de Educación Superior de Ensenada, Baja California (CICESE; Mexico), under internal project no. 644170.

Conflict of Interest

The authors declare that the research was conducted in the absence of any commercial or financial relationships that could be construed as a potential conflict of interest.

Publisher's Note

All claims expressed in this article are solely those of the authors and do not necessarily represent those of their affiliated organizations, or those of the publisher, the editors and the reviewers. Any product that may be evaluated in this article, or claim that may be made by its manufacturer, is not guaranteed or endorsed by the publisher.

Acknowledgments

This article is part of the doctoral project thesis of SP and the authors thank CONACYT for funding the doctoral fellowship (1086975).

Supplementary Material

The Supplementary Material for this article can be found online at:
https://www.frontiersin.org/articles/10.3389/feart.2021.716970/full#supplementary-material

References

Agusto, M., and Varekamp, J. (2016). "The Copahue Volcanic-Hydrothermal System and Applications for Volcanic Surveillance," in *Copahue Volcano, Active Volcanoes of the World*. Editors F. Tassi, O. Vaselli, and A. T. Caselli (Berlin Heidelberg: Springer), 199–238. doi:10.1007/978-3-662-48005-2_9

CrossRef Full Text | Google Scholar

Alvarado, G. E. (2009). Los volcanes de Costa Rica: Geología, historia, riqueza natural y su gente. *Univ. Estatal A Distancia* Vol. 32 (3). Costa Rica.

Google Scholar

Azimi, G., and Papangelakis, V. G. (2010). The Solubility of gypsum and Anhydrite in Simulated Laterite Pressure Acid Leach Solutions up to 250°C. *Hydrometallurgy* 102 (1-4), 1–13. doi:10.1016/j.hydromet.2009.12.009

CrossRef Full Text | Google Scholar

Barberi, F., Bertagnini, A., Landi, P., and Principe, C. (1992). A Review on Phreatic Eruptions and Their Precursors. *Hydrometallurgy* 102, 231–246. doi:10.1016/0377-0273(92)90046-G(

CrossRef Full Text | Google Scholar

Bernard, A., Escobar, C. D., Mazot, A., and Gutierrez, R. E. (2004). "The Acid Volcanic lake of Santa Ana Volcano, El Salvador," in *Natural Hazards in El Salvador*. Editors W. I. Rose, J. J. Bommer, D. L. López, M. J. Carr, and J. J. Major (Geological Society of America), Special paper, Vol. 375, 121–134. doi:10.1130/0-8137-2375-2.121

CrossRef Full Text | Google Scholar

Brantley, S. L., Borgiatt, A., Rowe, G., Fernández, J. F., and Reynolds, J. R. (1987). Poás Volcano Crater lake Acts as a Condenser for Acid Metal-Rich Brine. *Nature* 330, 470–472. doi:10.1038/330470a0

CrossRef Full Text | Google Scholar

Brown, G. C., Rymer, H., and Stevenson, D. (1991). Volcano Monitoring by Microgravity and Energy Budget Analysis. *J. Geol. Soc.* 148, 585–593. doi:10.1144/gsjgs.148.3.0585

CrossRef Full Text | Google Scholar

Brown, G., Rymer, H., Dowden, J., Kapadia, P., Stevenson, D., Barquero, J., et al. (1989). Energy Budget Analysis for Poás Crater lake: Implications for Predicting Volcanic Activity. *Nature* 339, 370–373. doi:10.1038/339370a0

CrossRef Full Text | Google Scholar

Capaccioni, B., Rouwet, D., and Tassi, F. (2017). HCl Degassing from Extremely Acidic Crater Lakes: Preliminary Results from Experimental Determinations and Implications for Geochemical Monitoring. *Geol. Soc. Lond. Spec. Publications* 437, 97–106. doi:10.1144/SP437.12

CrossRef Full Text | Google Scholar

Carr, M. J., Feigenson, M. D., Bolge, L. L., Walker, J. A., and Gazel, E. (2013). RU_CAGeochem, a Database and Sample Repository for Central American Volcanic Rocks at Rutgers University. *Earth Chem. Libr.* 1 (1), 43–48. doi:10.1594/IEDA/100403

CrossRef Full Text | Google Scholar

Christenson, B., and Tassi, F. (2015). “Gases in Volcanic lake Environments,” in *Volcanic Lakes*. Editors D. Rouwet, B. W. Christenson, F. Tassi, and J. Vandemeulebrouck (Heidelberg: Springer), 125–153. doi:10.1007/978-3-642-36833-2_5

CrossRef Full Text | Google Scholar

Christenson, B. W. (2000). Geochemistry of Fluids Associated with the 1995-1996 Eruption of Mt. Ruapehu, New Zealand: Signatures and Processes in the Magmatic-Hydrothermal System. *J. Volcanology Geothermal Res.* 97, 1–30. doi:10.1016/S0377-0273(99)00167-5

CrossRef Full Text | Google Scholar

Christenson, B. W., Reyes, A. G., Young, R., Moebis, A., Sherburn, S., Cole-Baker, J., et al. (2010). Cyclic Processes and Factors Leading to Phreatic Eruption Events: Insights from the 25 September 2007 Eruption through Ruapehu Crater Lake, New Zealand. *J. Volcanology Geothermal Res.* 191, 15–32. doi:10.1016/j.volgeores.2010.01.00810.1016/j.jvolgeores.2010.01.008

CrossRef Full Text | Google Scholar

Cigolini, C., Kudo, A. M., Brookins, D. G., and Ward, D. (1991). The Petrology of Poás Volcano Lavas: basalt-andesite Relationship and Their Petrogenesis within the Magmatic Arc of Costa Rica. *J. Volcanology Geothermal Res.* 48, 367–384. doi:10.1016/0377-0273(91)90052-2

CrossRef Full Text | Google Scholar

Colvin, A., Rose, W. I., Varekamp, J. C., Palma, J. L., Escobar, D., Gutierrez, E., et al. (2013). “Crater Lake Evolution at Santa Ana Volcano (El Salvador) Following the 2005 Eruption,” in *Understanding Open-Vent Volcanism and Related Hazards*. Editors W. I. Rose, J. L. Palma, H. D. Granados, and N. Varley (Boulder, CO: Geological Society of America), 23–43. doi:10.1130/2013.2498(02

CrossRef Full Text | Google Scholar

de Moor, J. M., Aiuppa, A., Pacheco, J., Avard, G., Kern, C., Liuzzo, M., et al. (2016). Short-period Volcanic Gas Precursors to Phreatic Eruptions: Insights from Poás Volcano, Costa Rica. *Earth Planet. Sci. Lett.* 442, 218–227. doi:10.1016/j.epsl.2016.02.056

CrossRef Full Text | Google Scholar

Delmelle, P., and Bernard, A. (1994). Geochemistry, Mineralogy, and Chemical Modeling of the Acid Crater lake of Kawah Ijen Volcano, Indonesia. *Geochimica et Cosmochimica Acta* 58, 2445–2460. doi:10.1016/0016-7037(94)90023-X

CrossRef Full Text | Google Scholar

Dutrizac, J. E. (2017). The Behaviour of the Rare Earth Elements during gypsum (CaSO 4 ·2H 2 O) Precipitation. *Hydrometallurgy* 174, 38–46. doi:10.1016/j.hydromet.2017.09.013

CrossRef Full Text | Google Scholar

Fischer, T. P., Ramírez, C., Mora-Amador, R. A., Hilton, D. R., Barnes, J. D., Sharp, Z. D., et al. (2015). Temporal Variations in Fumarole Gas Chemistry at Poás Volcano, Costa Rica. *J. Volcanology Geothermal Res.* 294, 56–70. doi:10.1016/j.jvolgeores.2015.02.002

CrossRef Full Text | Google Scholar

Giggenbach, W. F., and Glover, R. B. (1975). The Use of Chemical Indicators in the Surveillance of Volcanic Activity Affecting the Crater Lake on Mt Ruapehu, New Zealand. *Bull. Volcanol* 39, 70–81. doi:10.1007/BF02596947

CrossRef Full Text | Google Scholar

Hikov, A. (20152015). "Behaviour of Inert (Immobile) Elements in Extremely Acid Leaching: an Example from Asarel Porphyry Copper deposit," in GEOSCIENCES 2015, Proceedings of Jubilee national Conference (Sofia, 65–66. 10-11.12

Google Scholar

Hilton, D. R., Ram^|^Iacute;Rez, C. J., Mora-Amador, R., Fischer, T. P., F^|^Uuml;Ri, E., Barry, P. H., et al. (2010). Monitoring of Temporal and Spatial Variations in Fumarole Helium and Carbon Dioxide Characteristics at Po^|^aacute;s and Turrialba Volcanoes, Costa Rica (2001-2009). *Geochem. J.* 44, 431–440. doi:10.2343/geochemj.1.0085

CrossRef Full Text | Google Scholar

Inguaggiato, C., Burbano, V., Rouwet, D., and Garzón, G. (2017). Geochemical Processes Assessed by Rare Earth Elements Fractionation at "Laguna Verde" Acidic-Sulphate Crater lake (Azufral Volcano, Colombia). *Appl. Geochem.* 79, 65–74. doi:10.1016/j.apgeochem.2017.02.013

CrossRef Full Text | Google Scholar

Inguaggiato, C., Censi, P., Zuddas, P., Londoño, J. M., Chacón, Z., Alzate, D., et al. (2015). Geochemistry of REE, Zr and Hf in a wide range of pH and water composition: The Nevado del Ruiz volcano-hydrothermal system (Colombia). *Chem. Geology.* 417, 125–133. doi:10.1016/j.chemgeo.2015.09.025

CrossRef Full Text | Google Scholar

Inguaggiato, C., Iñiguez, E., Peiffer, L., Kretzschmar, T., Brusca, L., Mora-Amador, R., et al. (2018). REE Fractionation during the gypsum Crystallization in Hyperacid Sulphate-Rich Brine: The Poás Volcano Crater lake (Costa Rica) Exploited as Laboratory. *Gondwana Res.* 59, 87–96. doi:10.1016/j.gr.2018.02.022

CrossRef Full Text | Google Scholar

Inguaggiato, C., Pappaterra, S., Peiffer, L., Apollaro, C., Brusca, L., De Rosa, R., et al. (2020a). Mobility of REE from a Hyperacid Brine to Secondary Minerals Precipitated in a Volcanic Hydrothermal System: Kawah Ijen Crater lake (Java, Indonesia). *Sci. Total Environ.* 740, 140133–140214. doi:10.1016/j.scitotenv.2020.140133

PubMed Abstract | CrossRef Full Text | Google Scholar

Inguaggiato, C., Pérez García, M. Á., Meza Maldonado, L. F., Peiffer, L., Pappaterra, S., and Brusca, L. (2020b). Precipitation of Secondary Minerals in Acid Sulphate-Chloride Waters Traced by Major, Minor and Rare Earth Elements in Waters: The Case of Puracé Volcano (Colombia). *J. Volcanology Geothermal Res.* 407, 107106–107110. doi:10.1016/j.jvolgeores.2020.107106

CrossRef Full Text | Google Scholar

Kalacheva, E., Taran, Y., Kotenko, T.Y., Oi, T., Honda, T., et al. (20151993). Geochemistry and Solute Fluxes of Volcano-Hydrothermal Systems of Shiashkotan, Kuril IslandsLanthanoid Abundances of Acidic Hot spring and Crater lake Waters in the Kusatsu-Shirane Volcano Region, Japan. *J. Volcanology Geothermal ResearchGeochem. J.* 29627, 4019–5433. doi:10.1016/j.jvolgeores.2015.03.010Kikawada10.2343/geochemj.27.19

CrossRef Full Text | Google Scholar

Kikawada, Y., Uruga, M., Oi, T., and Honda, T. (2004). Mobility of Lanthanides Accompanying the Formation of Alunite Group Minerals. *J. Radioanal. Nucl. Chem.* 261 (3), 651–659. doi:10.1023/B:JRNC.0000037109.34238.cc

CrossRef Full Text | Google Scholar

Kilgour, G., V. Manville, V., Pasqua, F. D., A. Graettinger, A., Hodgson, K. A., and Jolly, G. E. (2010). The 25 September 2007 Eruption of Mount Ruapehu, New Zealand: Directed Ballistics, Surtseyan Jets, and Ice-Slurry Lahars. *J. Volcanology Geothermal Res.* 191 (12), 1–14. doi:10.1016/j.jvolgeores.2009.10.015

CrossRef Full Text | Google Scholar

Lewis, A. J., Palmer, M. R., Sturchio, N. C., and Kemp, A. J. (1997). The Rare Earth Element Geochemistry of Acid-Sulphate and Acid-Sulphate-Chloride Geothermal Systems from Yellowstone National Park, Wyoming, USA. *Geochimica et Cosmochimica Acta* 61, 695–706. doi:10.1016/S0016-7037(96)00384-5

CrossRef Full Text | Google Scholar

Manville, V. (2015). “Volcano-hydrologic Hazards from Volcanic Lakes,” in *Volcanic Lakes*. Editors D. Rouwet, B. W. Christenson, F. Tassi, and J. Vandemeulebrouck (Heidelberg: Springer), 21–71. doi:10.1007/978-3-642-36833-2_2

CrossRef Full Text | Google Scholar

Martínez, M., Fernández, E., Valdés, J., Barboza, V., Van der Laat, R., Duarte, E., et al. (2000). Chemical Evolution and Volcanic Activity of the Active Crater lake of Poás Volcano, Costa Rica, 1993–1997. *J. Volcanol. Geochem. Res.* 97, 127–141. doi:10.1016/S0377-0273(99)00165-1

CrossRef Full Text | Google Scholar

Martinez, M. (2008). *Geochemical Evolution of the Acidic Crater lake of Poás Volcano (Costa Rica): Insight into Volcanic-Hydrothermal Processes*. Thesis, Universiteit Utrecht: Ph.D., 162p.

Google Scholar

Michard, A. (1989). Rare Earth Element Systematics in Hydrothermal Fluids. *Geochimica et Cosmochimica Acta* 53, 745–750. doi:10.1016/0016-7037(89)90017-3

CrossRef Full Text | Google Scholar

Moor, J. M., Stix, J., Avard, G., Muller, C., Corrales, E., Diaz, J. A., et al. (2019). Insights on Hydrothermal-Magmatic Interactions and Eruptive Processes at Poás Volcano (Costa Rica) from High-Frequency Gas Monitoring and Drone Measurements. *Geophys. Res. Lett.* 46, 1293–1302. doi:10.1029/2018GL080301

CrossRef Full Text | Google Scholar

Mora Amador, R. A., Rouwet, D., Vargas, P., and Oppenheimer, C. (2019b). "The Extraordinary Sulfur Volcanism of Poás from 1828 to 2018," in *Poás Volcano (Costa Rica): The Pulsing Heart of Central America Volcanic Zone.* Editors F. Tassi, R. Mora-Amador, and O. Vaselli (Heidelberg): Springer), 45–78. doi:10.1007/978-3-319-02156-010.1007/978-3-319-02156-0_3

CrossRef Full Text | Google Scholar

Mora-Amador, R. A. (2010). *Peligrosidad volcánica del Poás (Costa Rica), basado en las principales erupciones históricas de 1834, 1910 y 1953–1955*. M.Sc. Thesis, Universidad de Costa Rica, 115.

Google Scholar

Mora-Amador, R. A., Rouwet, D., González, G., Vargas, P., and Ramírez, C. (2019a). "Poás Volcano," in *Poás Volcano (Costa Rica): The Pulsing Heart of Central America Volcanic Zone.* Editors F. Tassi, R. Mora-Amador, and O. Vaselli (Heidelberg): Springer), 45–78. doi:10.1007/978-3-319-02156-0

CrossRef Full Text | Google Scholar

Morton-Bermea, O., Aurora Armienta1, M., and Ramos, S. (2010). Rare-earth Element Distribution in Water from El Chichón Volcano Crater Lake, Chiapas Mexico. *GeofInt* 49 (1), 43–54. doi:10.22201/igeof.00167169p.2010.49.1.1474

CrossRef Full Text | Google Scholar

Ohba, T., Hirabayashi, J.-i., and Nogami, K. (2008). Temporal Changes in the Chemistry of lake Water within Yugama Crater, Kusatsu-Shirane Volcano, Japan: Implications for the Evolution of the Magmatic Hydrothermal System. *J. Volcanology Geothermal Res.* 178, 131–144. doi:10.1016/j.jvolgeores.2008.06.015

CrossRef Full Text | Google Scholar

Oppenheimer, C. (1992). Sulphur Eruptions at Volcán Poás, Costa Rica. *J. Volcanology Geothermal Res.* 49, 1–21. doi:10.1016/0377-0273(92)90002-U

CrossRef Full Text | Google Scholar

Oppenheimer, C. (1993). Thermal Distributions of Hot Volcanic Surfaces Constrained Using Three Infrared Bands of Remote Sensing Data. *Geophys. Res. Lett.* 20, 431–434. doi:10.1029/93GL00500

CrossRef Full Text | Google Scholar

OVSICORI (2021). Open Reports OVSICORI-UNA, Costa Rica. http://www.ovsicori.una.ac.cr.

Google Scholar

Pasternack, G. B., and Varekamp, J. C. (1997). Volcanic lake Systematics I. Physical Constraints. *Bull. Volcanology* 58, 528–538. doi:10.1007/s004450050160

CrossRef Full Text | Google Scholar

Peiffer, L., Taran, Y. A., Lounejeva, E., Solís-Pichardo, G., Rouwet, D., and Bernard-Romero, R. A. (2011). Tracing thermal Aquifers of El Chichón Volcano-Hydrothermal System (México) with 87Sr/86Sr, Ca/Sr and REE. *J. Volcanology Geothermal Res.* 205, 55–66. doi:10.1016/j.jvolgeores.2011.06.004

CrossRef Full Text | Google Scholar

Prosser, J. T., and Carr, M. J. (1987). Poás Volcano, Costa Rica: Geology of the summit Region and Spatial and Temporal Variations Among the Most Recent Lavas. *J. Volcanology Geothermal Res.* 33, 131–146. doi:10.1016/0377-0273(87)90057-6

CrossRef Full Text | Google Scholar

Rodríguez, A., and van Bergen, M. J. (2017). Superficial Alteration Mineralogy in Active Volcanic Systems: An Example of Poás Volcano, Costa Rica. *J. Volcanology Geothermal Res.* 346, 54–80. doi:10.1016/j.jvolgeores.2017.04.006

CrossRef Full Text | Google Scholar

Rouwet, D. (2021). “Forecasting and Planning for Volcanic Hazards, Risks, and Disasters,”. Editor P. Papale, 439, 471. Hazard and Disasters 2. doi:10.1016/C2018-0-02632-8

CrossRef Full Text | Google Scholar

Rouwet, D., Mora Amador, R. A., Sandri, L., Ramírez-Umaña, C., González, G., Pecoraino, G., et al. (2019). “39 Years of Geochemical Monitoring of Laguna Caliente Crater Lake, Poás: Patterns from the Past as Keys for the Future,” in *Poás Volcano (Costa Rica): The Pulsing Heart of Central America Volcanic Zone*. Editors F. Tassi, R. Mora-Amador, and O. Vaselli (Heidelberg): Springer), 213–233. doi:10.1007/978-3-319-02156-0_9

CrossRef Full Text | Google Scholar

Rouwet, D., Mora-Amador, R., Ramírez-Umaña, C. J., González, G., and Inguaggiato, S. (2017). “Dynamic Fluid Recycling at Laguna Caliente (Poás, Costa Rica) before and during the 2006-ongoing Phreatic Eruption Cycle (2005-10),” in *Geochemistry and Geophysics of Active Volcanic Lakes*. Editors T. Ohba, B. Capaccioni, and C. Caudron (Geological Society of London, Special Publications), 437, 73–96. doi:10.1144/SP437.11

CrossRef Full Text | Google Scholar

Rouwet, D., Taran, Y., Inguaggiato, S., Varley, N., and Santiago Santiago, J. A. (2008). Hydrochemical Dynamics of the "lake-spring" System in the Crater of El Chichón Volcano (Chiapas, Mexico). *J. Volcanology Geothermal Res.* 178, 237–248. doi:10.1016/j.jvolgeores.2008.06.026

CrossRef Full Text | Google Scholar

Rouwet, D., Tassi, F., Mora-Amador, R., Sandri, L., and Chiarini, V. (2014). Past, Present and Future of Volcanic lake Monitoring. *J. Volcanology Geothermal Res.* 272, 78–97. doi:10.1016/j.jvolgeores.2013.12.009

CrossRef Full Text | Google Scholar

Rowe, G. L., Brantley, S. L., Fernandez, J. F., and Borgia, A. (1995). The Chemical and Hydrologic Structure of Poa´s Volcano, Costa Rica. *J. Volcanology Geothermal Res.* 64, 233–267. doi:10.1016/0377-0273(94)00079-V

CrossRef Full Text | Google Scholar

Rowe, G. L., Brantley, S. L., Fernández, M., Fernández, J. F., Borgia, A., and Barquero, J. (1992a). Fluid-volcano Interaction in an Active Stratovolcano: the Crater lake System of Poás Volcano, Costa Rica. *J. Volcanology Geothermal Res.* 64, 233–267. doi:10.1016/0377-0273(92)90003-V

CrossRef Full Text | Google Scholar

Rowe, G. L., Ohsawa, S., Takano, B., Brantley, S. L., Fernández, J. F., and Barquero, J. (1992b). Using Crater Lake Chemistry to Predict Volcanic Activity at Poás Volcano, Costa Rica. *Bull. Volcanol* 54, 494–503. doi:10.1007/BF00301395

CrossRef Full Text | Google Scholar

Ruíz, P., Gazel, E., Alvarado, G. E., Carr, M. J., and Soto, G. J. (2010). Caracterización geoquímica y petrográfica de las unidades geológicas del macizo del volcán Poás, Costa Rica. *Rev. Geol. Amér. Cent.* 43, 37–66. doi:10.15517/RGAC.V0I43.3457

CrossRef Full Text | Google Scholar

Ruíz, P., Mana, S., Gazel, E., Soto, G. J., Carr, M. J., and Alvarado, G. E. (2019). "Geochemical and Geochronological Characterisation of the Poas Stratovolcano Stratigraphy," in *Poás Volcano (Costa Rica): The Pulsing Heart of Central America Volcanic Zone*. Editors F. Tassi, R. Mora-Amador, and O. Vaselli (Heidelberg): Springer), 13–43. doi:10.1007/978-3-319-02156-0_2

CrossRef Full Text | Google Scholar

Rymer, H., Locke, C. A., Borgia, A., Martínez, M., Brenes, J., Van der Laat, R., et al. (2009). Long-term Fluctuations in Volcanic Activity: Implications for Future Environmental Impact. *Terra Nova* 21, 304–309. doi:10.1111/j.1365-3121.2009.00885.x

CrossRef Full Text | Google Scholar

Sanford, W. E., Konikow, L. F., Rowe, G. L., and Brantley, S. L. (1995). Groundwater Transport of Crater-lake Brine at Poa´s Volcano, Costa Rica. *J. Volcanology Geothermal Res.* 64, 269–293. doi:10.1016/0377-0273(94)00080-Z

CrossRef Full Text | Google Scholar

Stix, J., and de Moor, J. M. (2018). Understanding and Forecasting Phreatic Eruptions Driven by Magmatic Degassing. *Earth Planets Space* 70, 83. doi:10.1186/s40623-018-0855-z

PubMed Abstract | CrossRef Full Text | Google Scholar

Takano, B., Saitoh, H., and Takano, E. (1994). Geochemical Implications of Subaqueous Molten Sulfur at Yugama Crater lake, Kusatsu-Shirane Volcano, Japan. *Geochem. J.* 28, 199–216. doi:10.2343/geochemj.28.199

CrossRef Full Text | Google Scholar

Takano, B., Suzuki, K., Sugimori, K., Ohba, T., Fazlullin, S. M., Bernard, A., et al. (2004). Bathymetric and Geochemical Investigation of Kawah Ijen Crater Lake, East Java, Indonesia. *J. Volcanology Geothermal Res.* 135, 299–329. doi:10.1016/j.jvolgeores.2004.03.008

CrossRef Full Text | Google Scholar

Taran, Y., Rouwet, D., Inguaggiato, S., and Aiuppa, A. (2008). Major and Trace Element Geochemistry of Neutral and Acidic thermal Springs at El Chichón Volcano, Mexico. *J. Volcanology Geothermal Res.* 178, 224–236. doi:10.1016/j.jvolgeores.2008.06.030

CrossRef Full Text | Google Scholar

Universidad de Costa Rica (2021). Reportes Volcanicos. Available at: https://rsn.ucr.ac.cr.

Google Scholar

van Hinsberg, V., Berlo, K., and Lowenstern, J. (2020). An Experimental Investigation of Interaction between Andesite and Hyperacidic Volcanic Lake Water. *Minerals* 10, 96–21. doi:10.3390/min10020096

CrossRef Full Text | Google Scholar

van Hinsberg, V., Berlo, K., Sumarti, S., Van Bergen, M., and Williams-Jones, A. (2010). Extreme Alteration by Hyperacidic Brines at Kawah Ijen Volcano, East Java, Indonesia: II. *J. Volcanology Geothermal Res.* 196, 169–184. doi:10.1016/j.jvolgeores.2010.07.004

CrossRef Full Text | Google Scholar

van Hinsberg, V., Vigouroux, N., Palmer, S., Berlo, K., Mauri, G., Williams-Jones, A., et al. (2017). "Element Flux to the Environment of the Passively Degassing Crater lake-hosting Kawah Ijen Volcano, Indonesia, and Implications for Estimates of the Global Volcanic Flux for Estimates of the Global Volcanic Flux," in *Geochemistry and Geophysics of Active Volcanic Lakes*. Editors T. Ohba, B. Capaccioni, and C. Caudron (London: Geological Society, Special Publications), 437, 9–34. doi:10.1144/SP437.21

CrossRef Full Text | Google Scholar

Vannucchi, P., and Morgan, J. P. (2019). "Overview of the Tectonics and Geodynamics of Costa Rica," in *Poás Volcano (Costa Rica): The Pulsing Heart of Central America Volcanic Zone*. Editors F. Tassi, R. Mora-Amador, and O. Vaselli (Heidelberg: Springer), 1–12. doi:10.1007/978-3-319-02156-0_1

CrossRef Full Text | Google Scholar

Varekamp, J. C., Ouimette, A. P., Herman, S. W., Flynn, K. S., Bermudez, A., and Delpino, D. (2009). Naturally Acid Waters from Copahue Volcano, Argentina. *Appl. Geochem.* 24 (2), 208–220. doi:10.1016/j.apgeochem.2008.11.018

CrossRef Full Text | Google Scholar

Varekamp, J. C., Pasternack, G. B., and Rowe, G. L. (2000). Volcanic lake Systematics II. Chemical Constraints. *J. Volcanology Geothermal Res.* 97, 161–179. doi:10.1016/S0377-0273(99)00182-1

CrossRef Full Text | Google Scholar

Varekamp, J. C. (2015). "The Chemical Composition and Evolution of Volcanic Lakes," in *Volcanic Lakes*. Editors D. Rouwet, B. W. Christenson, F. Tassi, and J. Vandemeulebrouck (Heidelberg: Springer), 93–123. doi:10.1007/978-3-642-36833-2_

CrossRef Full Text | Google Scholar

Vaselli, O., Tassi, F., Fischer, T. P., Tardani, D., Fernández, E., del Mar Martínez, M., et al. (2019). "The Last Eighteen Years (1998-2014) of Fumarolic Degassing at the Poás Volcano (Costa Rica) and Renewal Activity," in *Poás Volcano (Costa Rica): The Pulsing Heart of Central America Volcanic Zone*. Editors F. Tassi, R. Mora-Amador, and O. Vaselli (Heidelberg): Springer), 235–260. doi:10.1007/978-3-319-02156-010.1007/978-3-319-02156-0_10

CrossRef Full Text | Google Scholar

Vaselli, O., Tassi, F., Minissale, A., Montegrossi, G., Duarte, E., Fernández, E., et al. (2003). "Fumarole Migration and Fluid Geochemistry at Poás Volcano (Costa Rica) from 1998 to 2001," in *Volcanic Degassing. Special Publications*. Editors C. Oppenheimer, D. M. Pyle, and J. Barkley, 213, 247–262. doi:10.1144/GSL.SP.2003.213.01.15*Geol. Soc. Lond. Spec. Publications*

CrossRef Full Text | Google Scholar

von Frantzius, A. (1861). "Aporte al Conocimiento de los Volcanes de Costa Rica, Escalamiento al Volcán Poás, marzo 1860–1979," in *Volcán Poás*. Editor C. Vargas (San Jose: UNED), 11–34.

Google Scholar

Woitischek, J., Dietzel, M., Inguaggiato, C., Böttcher, M. E., Leis, A., Cruz, J. V., et al. (2017). Characterisation and Origin of Hydrothermal Waters at São Miguel (Azores) Inferred by Chemical and Isotopic Composition. *J. Volcanology Geothermal Res.* 346, 104–117. doi:10.1016/j.jvolgeores.2017.03.020

CrossRef Full Text | Google Scholar

Wood, S. A. (2006). Rare Earth Element Systematics of Acidic Geothermal Waters from the Taupo Volcanic Zone, New Zealand. *J. Geochemical Exploration* 89, 424–427. doi:10.1016/j.gexplo.2005.11.023

CrossRef Full Text | Google Scholar

Zlotnicki, J., Sasai, Y., Toutain, J. P., Villacorte, E. U., Bernard, A., Sabit, J. P., et al. (2009). Combined Electromagnetic, Geochemical and thermal Surveys of Taal Volcano (Philippines) during the Period 2005-2006. *Bull. Volcanol.* 71, 29–47. doi:10.1007/s00445-008-0205-2

CrossRef Full Text | Google Scholar